

RESEARCH ARTICLE

A bioinformatic analysis of the inhibin-betaglycan-endoglin/CD105 network reveals prognostic value in multiple solid tumors

Eduardo Listik¹ , Ben Horst^{1,2} , Alex Seok Choi¹, Nam. Y. Lee³, Balázs Gyórfy⁴, Karthikeyan Mythreye^{1*} 

1 Department of Pathology, Division of Molecular and Cellular Pathology, University of Alabama at Birmingham, Birmingham, Alabama, United States of America, **2** Department of Chemistry and Biochemistry, University of South Carolina, Columbia, South Carolina, United States of America, **3** Division of Pharmacology, Chemistry and Biochemistry, College of Medicine, University of Arizona, Tucson, Arizona, United States of America, **4** TTK Cancer Biomarker Research Group, Institute of Enzymology, and Semmelweis University Department of Bioinformatics and 2nd Department of Pediatrics, Budapest, Hungary

 These authors contributed equally to this work.

* mythreye@uab.edu



OPEN ACCESS

Citation: Listik E, Horst B, Choi AS, Lee N.Y, Gyórfy B, Mythreye K (2021) A bioinformatic analysis of the inhibin-betaglycan-endoglin/CD105 network reveals prognostic value in multiple solid tumors. PLoS ONE 16(4): e0249558. <https://doi.org/10.1371/journal.pone.0249558>

Editor: Donald P. Bottaro, Center for Cancer Research, UNITED STATES

Received: November 17, 2020

Accepted: March 21, 2021

Published: April 5, 2021

Peer Review History: PLOS recognizes the benefits of transparency in the peer review process; therefore, we enable the publication of all of the content of peer review and author responses alongside final, published articles. The editorial history of this article is available here: <https://doi.org/10.1371/journal.pone.0249558>

Copyright: © 2021 Listik et al. This is an open access article distributed under the terms of the [Creative Commons Attribution License](https://creativecommons.org/licenses/by/4.0/), which permits unrestricted use, distribution, and reproduction in any medium, provided the original author and source are credited.

Data Availability Statement: All relevant data are within the paper and its [Supporting information](#) files.

Abstract

Inhibins and activins are dimeric ligands belonging to the TGF β superfamily with emergent roles in cancer. Inhibins contain an α -subunit (*INH A*) and a β -subunit (either *INHBA* or *INHBB*), while activins are mainly homodimers of either β_A (*INHBA*) or β_B (*INHBB*) subunits. Inhibins are biomarkers in a subset of cancers and utilize the coreceptors betaglycan (*TGFBR3*) and endoglin (*ENG*) for physiological or pathological outcomes. Given the array of prior reports on inhibin, activin and the coreceptors in cancer, this study aims to provide a comprehensive analysis, assessing their functional prognostic potential in cancer using a bioinformatics approach. We identify cancer cell lines and cancer types most dependent and impacted, which included p53 mutated breast and ovarian cancers and lung adenocarcinomas. Moreover, *INH A* itself was dependent on *TGFBR3* and *ENG/CD105* in multiple cancer types. *INH A*, *INHBA*, *TGFBR3*, and *ENG* also predicted patients' response to anthracycline and taxane therapy in luminal A breast cancers. We also obtained a gene signature model that could accurately classify 96.7% of the cases based on outcomes. Lastly, we cross-compared gene correlations revealing *INH A* dependency to *TGFBR3* or *ENG* influencing different pathways themselves. These results suggest that inhibins are particularly important in a subset of cancers depending on the coreceptor *TGFBR3* and *ENG* and are of substantial prognostic value, thereby warranting further investigation.

Introduction

Inhibins and activins are dimeric polypeptide members of the TGF- β superfamily, discovered initially as regulators of follicle-stimulating hormone (FSH) [1–9]. Activins are homodimers utilizing different isoforms of the monomeric β_A or β_B subunits located on different

Funding: KM, R01CA219495, NCI <https://www.cancer.gov> and BG, 2018-2.1.17-TET-KR-00001, 2018-1.3.1-VKE-2018-00032 National Research, Development and Innovation Office Hungary (<https://ec.europa.eu/growth/tools-databases/regional-innovation-monitor/organisation/national-research-development-and-innovation-office>). The funders had no role in study design, data collection and analysis, decision to publish, or preparation of the manuscript.

Competing interests: NO authors have competing interests.

chromosomes [10–12]. Inhibin is a heterodimer of an α subunit (*INHA*) and a β subunit (either β_A , *INHBA*, or β_B , *INHBB*). Thus the inhibin naming reflects the β subunit in the heterodimer: inhibin A (α/β_A) and inhibin B (α/β_B), respectively [8, 13–16].

Activins, signal primarily through the transcriptional proteins SMAD2/3, much like TGF- β [17, 18]. Initial receptor binding of activin occurs via type II serine-threonine kinase receptors (ActRII or ActRIIB). These then recruit and phosphorylate type I serine-threonine kinase receptors (ActRIB/Alk4 or ActRIC/Alk7) leading to subsequent phosphorylation of SMAD2/3 [8, 17, 19–22]. In multiple tissues, activin signaling is antagonized by inhibin [23]. Thus, the biological and pathological function of activin is directly impacted by the relative levels of the mature α subunit. Inhibins, however, have a much lower affinity for the type II receptors compared to activins themselves. The affinity can be greatly enhanced by the presence of the Type III TGF β receptor, betaglycan (*TGFBR3*), which binds inhibin's α subunit with high affinity [8, 19, 23, 24]. Thus the most established mechanism of antagonism by inhibin, is via its ability to competitively recruit ActRII preventing activin induced downstream signaling in a betaglycan-dependent manner [8, 19, 23, 24]. This competition model does not allow for direct inhibin signaling. However, conflicting reports on the presence of a separate high affinity inhibin receptor [25, 26], recently discovered interactions of the α subunit with the Type I receptor Alk4 [24], and our recent findings on the requirement of the alternate Type III TGF- β co-receptor endoglin (*ENG/CD105*) for inhibin responsiveness in endothelial cell function [27] suggest complex roles for inhibins themselves.

Betaglycan and endoglin, are both coreceptors of the TGF- β superfamily with broad structural similarities [28–30], including glycosylation in the extracellular domain (ECD), a short cytoplasmic domain and common intracellular interacting partners [31–36]. Sequence analysis of betaglycan and endoglin reveal the highest shared homology in the transmembrane (73%) and cytoplasmic domains (61%), with the most substantial difference being in the ECD sequence that impacts ligand binding [28–30, 37–39]. Both betaglycan and endoglin knockouts (KOs) are lethal during embryonic development due to heart and liver defects and defective vascular development, respectively, highlighting the shared physiological importance of these coreceptors [40–43]. In contrast to the above-described similarities, betaglycan is more widely expressed in epithelial cells, while endoglin is predominantly expressed in proliferating endothelial cells [44–46].

In cancer, betaglycan and endoglin impact disease progression by regulating cell migration, invasion, proliferation, differentiation, and angiogenesis in multiple cancer models [34, 47–52]. Betaglycan can act as a tumor suppressor in many cancer types and its expression is lost in several primary cancers [53–55]. However, elevated levels of betaglycan have also been reported in colon, triple-negative breast cancers and lymphomas, with a role in promoting bone metastasis in prostate cancer [56], indicating contextual roles for betaglycan in tumor progression [48, 57, 58]. Endoglin is crucial to angiogenesis, and increased endoglin and tumor micro-vessel density is correlated with decreased survival in multiple cancers [50, 59]. Evidence in ovarian cancer [60, 61] also suggests that endoglin expression may impact metastasis. Inhibins have been robustly implicated in cancer, and much like other TGF- β members may have dichotomous, context-dependent effects [62–69]. Inhibins are early tumor suppressors, as the *INHA*^{-/-} mice form spontaneous gonadal and granulosa cell tumors [62]. However, elevated levels of inhibins in multiple cancers are widely reported [63–66, 70, 71]. Active roles for inhibins in promoting late stage tumorigenesis, in part via effects on angiogenesis, have also been reported in both prostate cancer [72] and more recently in ovarian cancer [27].

Inhibins have been widely used as a diagnostic marker for a subset of cancers [70, 71, 73] and both betaglycan and endoglin have been evaluated as therapeutic strategies in cancer. TRC-105, a monoclonal antibody against endoglin, was tested in twenty-four clinical trials

[74–97]. Current data also suggest benefits of combining anti-endoglin along with checkpoint inhibitors [98]. Similarly a peptide domain of betaglycan called p144 and soluble betaglycan have been tested in multiple cancer types as an anti-TGF- β treatment strategy that decreases tumor growth, angiogenesis, metastasis, and augments immunotherapy [99–106].

Prior and emerging studies reveal the dichotomous functions of inhibin's on cancer depending on either betaglycan [8, 19, 23, 24] or endoglin [27]. Hence, further characterization of the relationship between inhibins-betaglycan-endoglin is vital. This study seeks to provide such prescient information by evaluating the significance, impact, and predictive value of this specific network (*INHA*, *INHBA*, *INHBB*, *TGFBR3*, and *ENG*) by utilizing publicly available genomic and transcriptomic databases.

Materials and methods

Public databases data mining

Clinical data, gene expression alterations, and normalized expression data of RNA-seq were obtained from cBioPortal [107, 108]. All available studies were assessed for copy number alterations (CNA) and a subset of cancer for mRNA data (Breast Invasive Carcinoma, Glioblastoma, Lower-grade glioma, Cervical Squamous Cell Carcinoma, Stomach Adenocarcinoma, Head and Neck Squamous Cell Carcinoma, Kidney Renal Clear Cell and Renal Papillary Cell Carcinomas, Liver Hepatocellular Carcinoma, Lung Adenocarcinoma, Ovarian Serous Cystadenocarcinoma, Prostate Adenocarcinoma, Uterine Corpus Endometrial Carcinoma). The results shown here are partly based upon data generated by the TCGA Research Network: <https://www.cancer.gov/tcga>. Survival data was generated from either KM Plotter [109] or cBioportal (i.e., brain cancers). KM Plotter data for breast, ovarian, lung, and gastric cancer the survival analysis was derived using available gene chip data sets. All others were derived using the RNA-Seq Pan-cancer data sets. The Affymetrix Probe IDs used in gene chip analysis in KM Plotter were: *INHA* (210141_s_at), *INHBA* (204926_at), *INHBB* (205258_at), *TGFBR3* (204731_at), and *ENG* (201808_s_at). Brain cancer data was generated from TCGA Pan Cancer Atlas 2018 dataset for glioblastoma and low-grade glioma. Overall survival (OS) was assessed for all cancer types except ovarian cancer (progression-free survival, PFS) and breast cancer (relapse-free survival, RFS). Gene expression was split into high and low using the median expression. Log-rank statistics were used to calculate the p-value and Hazard ratio (HR).

Analysis of gene predictiveness to pharmacological treatment

Gene predictive information on treatment regiments was obtained from ROC Plotter (<http://www.rocplot.org/>) [110]. Gene expression for the analyzed genes was compared using the Mann-Whitney U test. Receiver Operating Characteristic (ROC) plots and significance was also computed. ROC curves were compared using Area Under the Curve (AUC) values, and values above 0.6 with a significant p value were considered acceptable [110]. ROC plot assessment was performed in all pre-established categories in ROC Plotter (i.e., breast and ovarian cancers, and glioblastoma). In breast cancer, subtypes (i.e., luminal A, luminal B, triple-negative, HER2⁺) were also analyzed separately. Genes of interest were analyzed for complete pathological response in different pharmacological treatments. All available treatment options were investigated including, taxane, anthracycline, platin and temozolomide. Outliers were set to be removed in this analysis and only genes with a false discovery rate (FDR) below 5% were considered.

Clustering strategies for genes signatures

From the normalized expression data from RNA-seq studies, the Spearman's ρ coefficient was obtained for *INHA*, *TGFBR3*, and *ENG*. These data were clustered through a Euclidean clustering algorithm using Perseus 1.6.5.0 (MaxQuant). Clusters containing high and low correlations sets were isolated and compared in a pair-wise fashion. The derived genes obtained were checked for protein interaction in BioGRID (thebiogrid.org) [111], and later included in pathway analysis, as described in section 2.5. All plots were performed in GraphPad Prism 8.0.

Gene signature modeling for prognostics

Gene signature modeling was performed using binary probit regression for each set of cancer types related to *INHA*, *TGFBR3*, *ENG* (S5 Table), and their respective outcomes (i.e., positive, 1; or negative, 0). The regression was iterated for presenting only significant elements in the following model:

$$\Pr(Y = 1|x_1, \dots, x_k) = \Phi(\beta_0 + \sum_{i=1}^k \beta_i x_i)$$

in which x_i are RNA-seq V2 RSEM expression data for each gene, β_i are obtained coefficients from this regression, Φ is the cumulative normal distribution function. Probability values closer to 1 indicate a positive outcome, while values close to 0, indicate a negative outcome. Postestimation of specificity and sensitivity was also implemented. All regression studies were performed in Stata/SE 16.0.

Pathway assessment

For pathway analysis, DAVID Bioinformatics Resources 6.8 was used to acquire compiled data from the KEGG Pathway Database [112]. Genes for the analysis were annotated to map to human pathways. The significant outputs were then assessed for the percentage of genes from analyzed sets and their relevance. To compare pathways between two sets, a pathway significance value ratio ($-\log_{10}R$), in which R is the ratio, was analyzed. Only pathways with an FDR value below 5% were considered.

Gene dependency analysis

Gene dependency of *INHA*, *TGFBR3*, *INHBA*, *INHBB*, and *ENG* was analyzed using the Dep-Map portal (www.depmap.org) [113]. Gene expression from Expression Public20Q1 (accessed between March and April 2020) were compared to the cell line database from CRISPR (Avana) Public20Q1 and Combined RNAi (Broad, Novartis, Marcotte). Gene effect values of less than or equal to -0.5 were used to select dependent genes.

To analyze gene co-dependency, Expression Public20Q1 was compared to all CRISPR and RNAi databases. A gene was considered dependent when correlations between datasets displayed similar trends. Each dependent gene-set was compared between *INHA*, *TGFBR3*, *INHBA*, *INHBB*, and *ENG* to count duplicates. The number of dependent genes were plotted as a Venn diagram.

Results

Inhibins and activins are altered in human cancer

We and others reported previously diverse roles for members of the inhibin/activin family in cancer [8, 27, 114–117]. Our and prior mechanistic studies in cancer indicate a strong

dependency of inhibin function on betaglycan and endoglin [24, 27, 118–121]. To begin to evaluate the impact of this relationship more broadly in cancers we analyzed gene alterations including mutations, amplifications, and deletions for the genes encoding inhibin/activin subunits (Fig 1a) *INHA*, *INHBA*, *INHBB*, and the key coreceptors—*TGFBR3*, and *ENG* in all public datasets available in cBioPortal (Fig 1b, S1 Table). While *INHBC* and *INHBE* are activin subunits, these were excluded from the analysis as they have not been demonstrated to form heterodimers with *INHA* [122].

Percentage of patients from the whole cohort that possessed any of the alterations either by themselves or concomitantly was analyzed. We find that melanoma (16.26%), endometrial (13.16%), esophagogastric (10.85%), and lung (10.69%) cancers revealed the highest alterations for the genes. The alterations for the genes varied, with *INHBA* and *TGFBR3* exhibiting higher rates of alterations (0–5.65% and 0.17–3.91% respectively) that also varied by cancer type. The range for *INHA*, *INHBB*, and *ENG* was found to be between 0–2.38%, 0–2.62%, and 0–3.23% respectively (Fig 1b).

In comparing expression levels of each of the genes in the same TCGA datasets as in Fig 1b, we find that overall *ENG* is the most highly expressed gene (Fig 1c) with variance among different cancer types (e.g., lower-grade glioma and cervical vs. renal clear cell and lung adenocarcinoma, $p < 0.0001$) and subtypes (e.g., luminal A vs. luminal B breast cancers, $p < 0.0001$). Interestingly, *TGFBR3* expression differed most notably between glioblastoma and lower-grade gliomas ($p < 0.0001$). Breast cancers exhibited higher expression as compared to ovarian and endometrial ($p < 0.0001$) cancers. *INHBB* in contrast was mostly expressed in renal clear cell and hepatocellular carcinomas, which differs from renal papillary cell carcinoma and cervical cancer ($p < 0.0001$). Both *INHBA* and *INHA* were the least expressed as compared to the others (Fig 1c). Exceptions were head and neck and esophagogastric cancers that had high expression of *INHBA* and lung adenocarcinoma and renal clear cell carcinoma that had high expression of *INHA*.

While the above analysis examined patient tumors, we next examined cell lines as a way to delineate model systems for future studies. For these analyses, we used the DepMap project (www.depmap.org) [113] which is a comprehensive library of human genes that have been either knocked down or knocked out through CRISPR technology in 1,776 human cell lines representing multiple cancer types [123–125]. Dependency scores representing the probability of queried gene dependency for each cell line and thereby cancer type is obtained [126]. Here, we find that the ligand encoding gene *INHA* displayed higher dependency than the activin subunit isoforms *INHBA* or *INHBB* or either receptors *TGFBR3* or *ENG* (Fig 1d). Notably, esophageal, gastric, and ovarian cancers had the highest dependency results for *INHA* ($\geq 14\%$) consistent with the alterations seen in Fig 1c. Within these cancers, *INHBA* exhibited higher dependency values in ovarian cancer (6%) albeit not as high as *INHA*. Besides *INHBB* in myeloma (6%), no other notable dependency relationships were observed.

In an attempt to identify genes most impacted by alteration to each of the individual genes, we examined how RNAi and CRISPR interventions would affect their correlation to specific genes. Those similarly affected by these techniques were found to be dependent on the investigated set of genes. We find that *ENG* exhibited the highest number of dependent genes (Fig 1e, $n = 71$) followed by *INHBA* (57), *INHBB* (49), *TGFBR3* (44) and *INHA* (30) (Fig 1e, S1 Table). Interestingly, only a total of 5 genes were commonly dependent between *INHA* and the other genes (Fig 1e, *MAX* with *INHBA* and *GRPEL1*, *SF3B4*, *ESR1*, and *TFAP2C* with *INHBB*). *INHBA* on the other hand had several common dependent genes most notably 13 genes were common with *ENG* dependency (e.g., *VCL*, *TLN1*, and *LYPD3*).

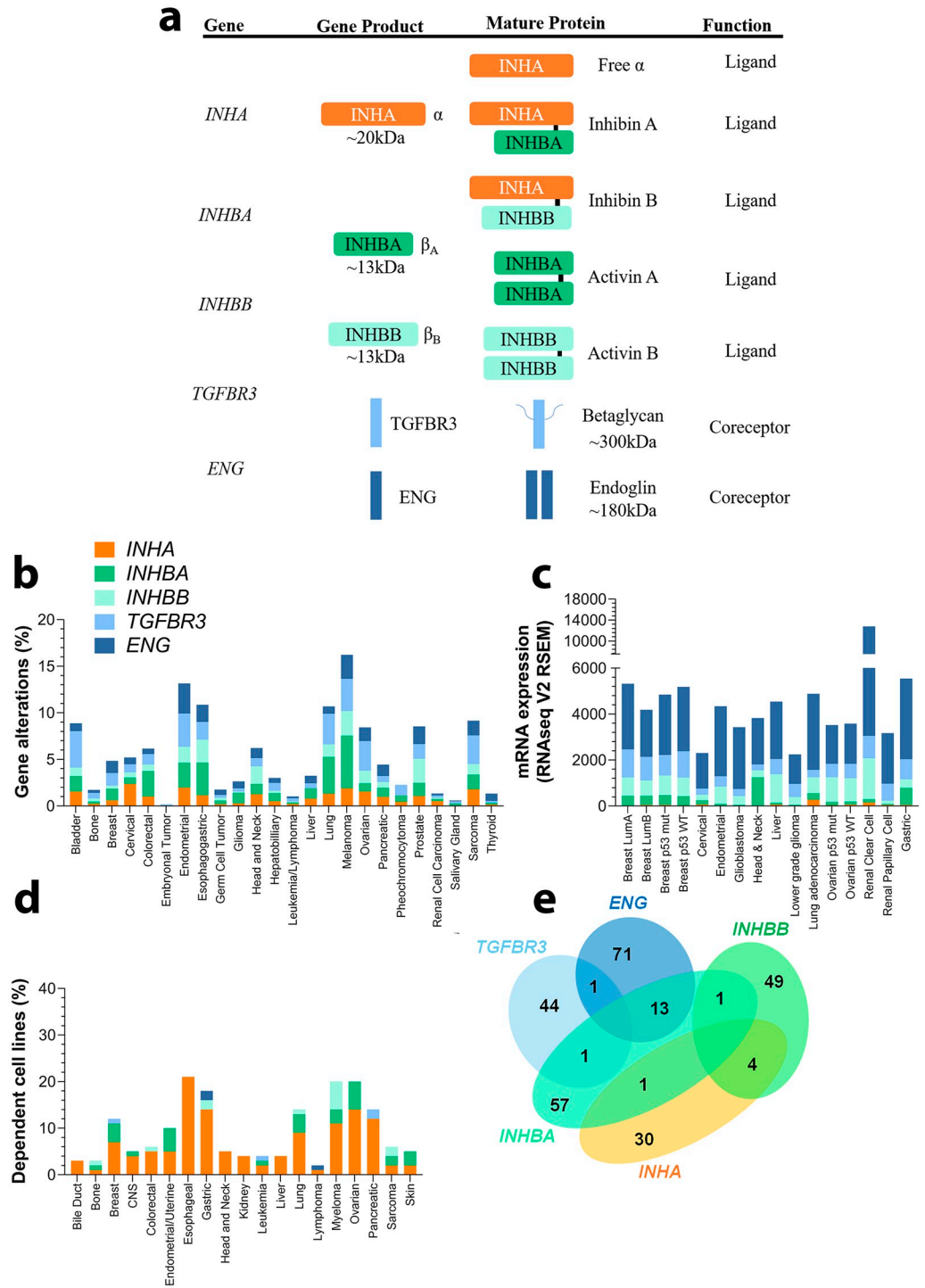


Fig 1. Expression and gene alterations of inhibin and activins. (a) Genes encoding *INHBA*, *INHBA*, and *INHBA* produce monomeric α and β subunits. These subunits combine to form either homo or heterodimers representing mature inhibin A, inhibin B, activin A, and activin B. (b) TCGA base analysis of gene alteration frequencies of *INHBA*, *INHBA*, *INHBB*, *TGFBR3*, and *ENG*. (c) Analysis of gene expression levels, also from TCGA sets, of the same genes as in (b) in a subset of cancer types and subtypes. Analysis included 16 studies and 6258 samples. (d) DepMap analysis of cell line dependency from indicated cancer types on each of the genes in (b). (e) Venn diagram illustrating the number of common dependent genes for each gene in (b). All numeric data are available in [S1 Table](#). Abbreviations—CNS: Central Nervous System; LumA: Luminal A; LumB: Luminal B; mut: mutated; WT: wild-type.

<https://doi.org/10.1371/journal.pone.0249558.g001>

Effect of inhibins and the coreceptors on patient survival varies by cancer type

Since alterations in expression of inhibin, activin, *TGFBR3* and *ENG* exist in human cancers and prior studies have implicated each of these in patient outcomes [27, 52, 59, 71, 114, 127–130]; we conducted a comprehensive analysis of each of these genes on overall survival (OS), progression-free survival (PFS), or relapse free survival (RFS) in a broad panel of cancers. The goal here was to identify the patients and cancer types most impacted by changes in gene expression. Analysis was conducted using datasets in KM Plotter (Figs 2 and 3, summarized in S2 Table) [109]. For ovarian cancer data sets, only p53 mutated ovarian cancers were included. Patients in KM plotter with p53 mutation status known showed 83% were mutated, cBioportal data sets showed 82.5% frequency of p53 mutation, and it has been reported that over 90% of ovarian cancers present p53 mutations. We find that not all cancers are equally impacted. Of note, we find that in both breast and ovarian cancers all five genes were either positive predictors of survival or non-predictive except *INHBB* in breast (HR = 1.06, $p = 0.034$) and *INHBA* in ovarian (HR = 1.16, $p = 0.047$) (Fig 2). However, in p53 mutated cancers, *INHA* was a strong negative predictor of survival for both breast and ovarian cancers (HR = 1.99, $p = 0.0056$ and HR = 1.55, $p = 0.0039$, respectively), along with *ENG* in ovarian cancer (HR = 1.36, $p = 0.0098$, Figs 2 and 3). Additionally, in lung cancers, *INHA* and *ENG* differed from *TGFBR3*, as *INHA* (HR = 1.26, $p = 0.00029$) and *ENG* (HR = 1.20, $p = 0.0056$) were both negative predictors of survival while *TGFBR3* (HR = 0.65, $p = 3.4E-7$) was a strong positive predictor of survival (Fig 2). Specifically, we find that *INHA* and *ENG* are robust predictors of poor survival in lung adenocarcinomas but not in squamous cell carcinomas (Figs 2 and 3). Gastric cancers represent another robust cancer type where all five genes were negatively correlated with survival (Figs 2 and 3). Since *HER2* expression is a frequent abnormality in gastric cancer [131], we examined if there were any differences in survival associated with *HER2* expression. All five genes in both *HER2*⁺ and *HER2*⁻ gastric cancers, except *INHBA* in *HER2*⁻ gastric cancers, were negatively correlated with survival (Fig 2). In kidney cancers, *INHA* was a negative predictor of survival in both renal clear cell and renal papillary cell carcinoma (Figs 2 and 3), consistent with prior findings [27]. *TGFBR3* was a strong positive predictor of survival in both renal clear cell carcinoma (HR = 0.46, $p = 2.1E-7$) and renal papillary cell carcinoma (HR = 0.53, $p = 0.042$, Figs 2 and 3). *ENG* (HR = 0.51, $p = 8.6E-6$) was a positive predictor of survival in renal clear cell carcinoma but not significantly associated with survival in renal papillary cell carcinoma (Fig 2). Finally, in brain cancers, *INHA* was a negative predictor of survival in glioblastoma but a positive predictor in low-grade gliomas (Fig 2). Of note, *ENG* appeared to have a lower range of HR values compared to *INHA* and *TGFBR3*. *INHBA* and *INBBB* were not as significantly correlated with survival as *INHA*, *ENG*, and *TGFBR3*. *INHBA* was significantly correlated with 8 cancer types while *INHBB* was significantly correlated with 9. *INHBA* and *INHBB* showed similar correlations with survival in gastric cancers, specifically *HER2*⁺, and renal papillary cell carcinoma (Fig 2). *INHBA* and *INHBB* showed opposing effects however in liver cancer where *INHBA* (HR = 0.62, $p = 0.0086$) was a strong positive predictor but *INHBB* (HR = 1.52, $p = 0.025$) was a potent negative predictor (Fig 2).

Since inhibin's biological functions have been shown to be dependent on the coreceptors *TGFBR3* and *ENG* [24, 27, 118–121], we examined the impact of *INHA* based on the expression levels of each of the co-receptor (Table 1). In this analysis, we find that that when separating patients into high or low expressing *TGFBR3* or *ENG* groups (Table 1) in p53 mutated breast cancers, where *INHA* is a negative predictor of survival in all patients (Fig 2), *INHA* was only a predictor of poor survival in patients with low *TGFBR3* (HR = 2.29, $p = 0.015$) or low *ENG* (HR = 2.24, $p = 0.035$). Interestingly, this trend was also repeated in renal clear cell

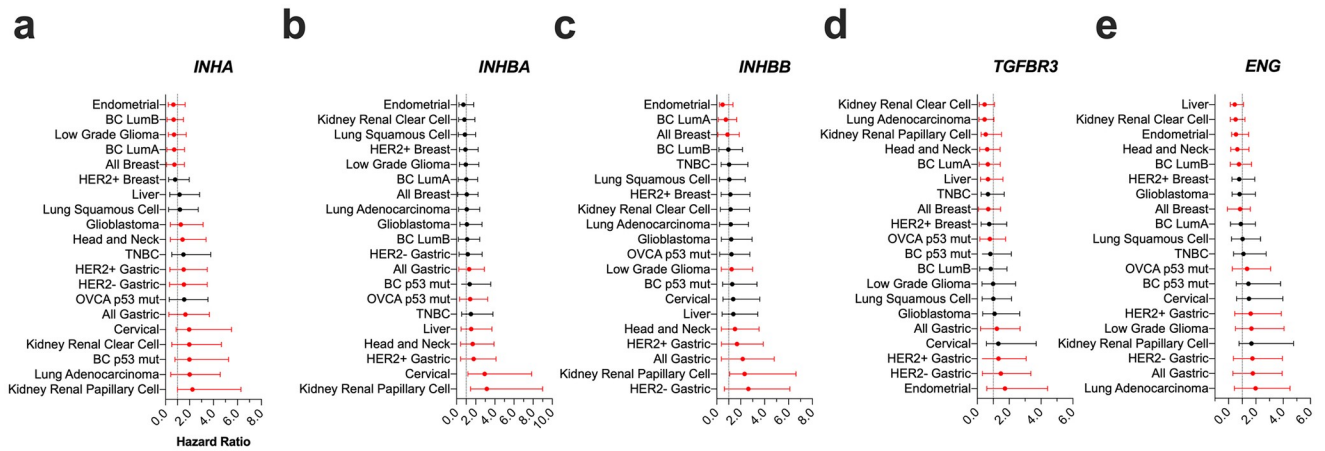


Fig 2. Impact of *INHA*, *INHBA*, *INHBB*, *TGFBR3*, and *ENG* on patient survival in indicated cancers. (a) Forest Plot with Hazard Ratios (HR) of indicated genes generated from KM Plotter or data from cBioportal. Black dots represent HR that are not statistically significant ($p > 0.05$) and red dots represent HR that are statistically significant ($p < 0.05$). All numeric data are available in [S2 Table](#).

<https://doi.org/10.1371/journal.pone.0249558.g002>

carcinoma, where *INHA* was only a predictor of survival in *TGFBR3* low (HR = 2.75, $p = 9.0E-06$) and *ENG* low (HR = 2.6, $p = 2.5E-06$, [Table 1](#)). In contrast to breast and renal clear cell cancers where *TGFBR3* and *ENG* both impacted the effect of *INHA* on survival, *TGFBR3* levels did not change *INHA*'s impact on p53 mutated serous ovarian cancers ([Table 1](#)). In *ENG* high p53 mutated serous ovarian cancer patients, *INHA* had a more significant negative prediction outcome (HR = 2.12, $p = 1.8E-6$) compared to *ENG* low (HR = 0.8, $p = 0.18$, [Table 1](#)). Similar outcomes were observed in lung adenocarcinomas with respect to *TGFBR3*, where *INHA* remained a strong negative predictor of survival in patients regardless of *TGFBR3* expression levels ([Table 1](#)). However, *INHA* remained a robust negative predictor of survival in lung

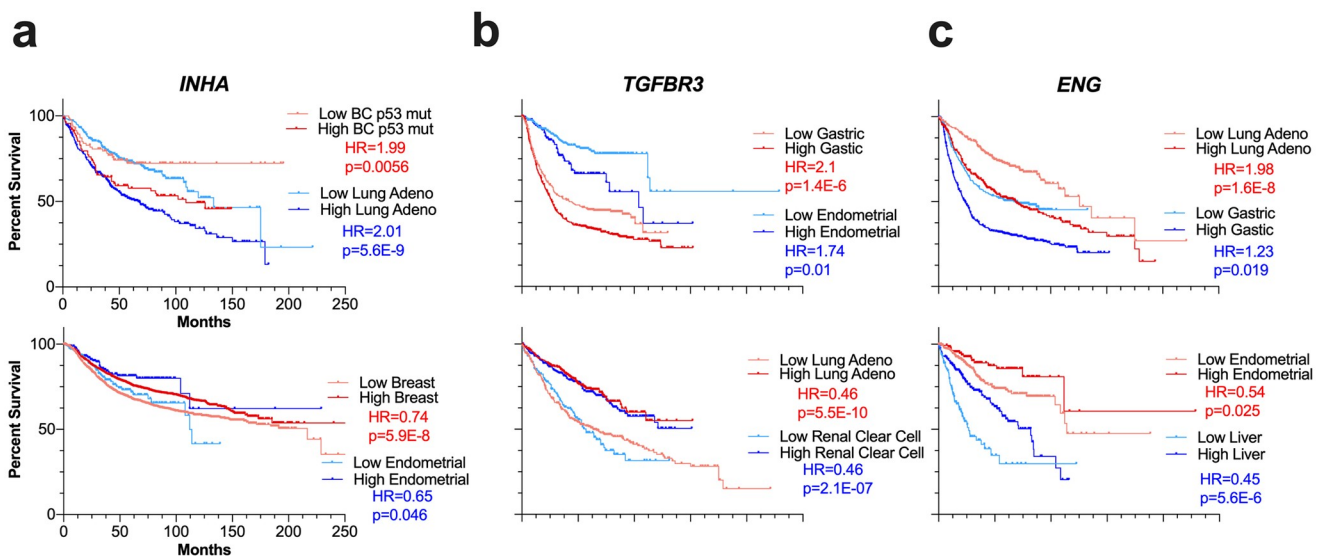


Fig 3. Representative Kaplan Meier curves for *INHA*, *TGFBR3*, and *ENG*. Event-free survival in indicated cancers using median to separate expression (lighter shade indicates bottom patients expressing bottom 50% and darker shade top 50%). Survival curves represent OS for all cancers except breast cancer (RFS) and ovarian cancer (PFS). Top plots show cancer types where the gene is a negative predictor of survival, and bottom plots show cancer types where the gene is a negative predictor.

<https://doi.org/10.1371/journal.pone.0249558.g003>

Table 1. p values and Hazard Ratios (HR) from survival curves assessing the relationship between *TGFBR3/ENG* and *INHA* on patient survival.

Type	Subtype	Variable	<i>INHA</i>	<i>TGFBR3</i>	<i>INHA and TGFBR3</i>	<i>INHA in High TGFBR3 Patients</i>	<i>INHA in Low TGFBR3 Patients</i>
Breast [#]	All	p value	5.9E-8	4E-11	4.5E-12	.00026	5.9E-6
		Hazard Ratio (HR)	.74	.69	.68	.74	.74
	p53 Mutated	p value	.0056	.41	.82	.27	.015
		Hazard Ratio (HR)	1.99	.82	.95	1.5	2.29
Ovarian*	p53 Mutated	p value	.00039	.039	.1	.021	.00075
		Hazard Ratio (HR)	1.55	.79	.83	1.51	1.74
Lung	All	p value	.00029	3.4E-7	1.4E-6	4.4E-5	.18
		Hazard Ratio (HR)	1.26	.65	.73	1.49	1.12
	Adenocarcinoma	p value	5.6E-9	5.5E-10	3.1E-7	1.7E-5	1.6E-8
		Hazard Ratio (HR)	2.01	.46	.53	2.49	1.98
Kidney	Renal Clear Cell	p value	7.1E-06	2.1E-7	3.3E-05	.2	9.0E-06
		Hazard Ratio (HR)	1.98	.46	.53	1.42	2.75
Type	Subtype	Variable	<i>INHA</i>	<i>ENG</i>	<i>INHA and ENG</i>	<i>INHA in High ENG Patients</i>	<i>INHA in Low ENG Patients</i>
Breast [#]	All	p value	5.9E-8	.0014	7.4E-6	.0043	.0027
		Hazard Ratio (HR)	.74	.84	.78	.79	.79
	p53 Mutated	p value	.0056	.12	.057	.26	.035
		Hazard Ratio (HR)	1.99	1.46	1.6	.69	2.24
Ovarian*	p53 Mutated	p value	.00039	.0098	.00091	1.8E-6	.18
		Hazard Ratio (HR)	1.55	1.36	1.49	2.12	.8
Lung	All	p value	.00029	.0056	.063	.47	5.8E-8
		Hazard Ratio (HR)	1.26	1.2	1.13	1.07	1.66
	Adenocarcinoma	p value	5.6E-9	1.6E-8	5.6E-12	.14	.00041
		Hazard Ratio (HR)	2.01	1.98	2.3	1.25	2.12
Kidney	Renal Clear Cell	p value	7.1E-06	8.6E-6	4.5E-05	.072	2.5E-06
		Hazard Ratio (HR)	1.98	.51	.53	1.53	2.6

Survival curves were generated in KM Plotter for all cancer types. Survival curves represent overall survival, progression free survival (marked with *), or relapse free survival (marked with #) for patients expressing high or low mRNA (split by median) of the indicated gene.

<https://doi.org/10.1371/journal.pone.0249558.t001>

adenocarcinomas patients expressing low *ENG* (HR = 2.12, p = 0.00041) but was not significant in *ENG* high expressing patients (HR = 1.25, p = 0.14) (Table 1).

Together, these findings suggest that *INHA* expression as a predictive tool for survival is influenced by the coreceptors *ENG* and *TGFBR3* in renal clear cell, lung, and p53 mutated breast and ovarian cancers. *INHA* is dependent on these coreceptors in all breast and ovarian cancers.

Inhibins and activins can predict response to chemotherapy in luminal A breast cancer

We next evaluated the pathological response based classification for each of the genes using the receiver operating characteristic (ROC) plotter (www.rocplot.org) to validate and rank *INHA*, *INHBA/B*, *TGFBR3* and *ENG* as predictive biomarker candidates [110]. In a ROC analysis, an area under the curve (AUC) value of 1 is a perfect biomarker and an AUC of 0.5 corresponds to no correlation at all. We first entered all genes to allow for FDR calculation for each gene at FDR cutoff of 5% (S3 Table). We next examined individual genes and find that in luminal A breast cancers *ENG*, *TGFBR3*, *INHA*, and *INHBA*, were better performing as compared

to *INHBB* particularly for taxane or anthracycline based chemotherapy regimens. ROC plots for the two regimens are displayed in Fig 4 and S3 Table.

Both *ENG* and *TGFBR3* were predictive in other cancer types as well (S3 Table). Specifically, while *ENG* performed better in taxane treatments in *HER2*⁺ breast cancer subtype, *TGFBR3* performed better for taxane regimens in triple-negative breast cancer (TNBC) and serous ovarian cancer. Interestingly, examining expression (Fig 4b) revealed that in the same luminal A breast cancers *INHA*, *ENG* and *INHBA* are less expressed in responders to pharmacological treatment while *TGFBR3* is more expressed in these responder groups (Fig 4b). Similar trends for *TGFBR3* expression were seen in TNBC and serous ovarian cancer groups where *TGFBR3* was more expressed in the responders' group for taxane regimens. *ENG* was also more expressed in *HER2*⁺ breast cancer patients who respond to taxane therapy, which was opposite to the luminal A subtype expression levels (Fig 4b). Full data for the ROC curve assessment is available in S3 Table. In summary *INHA*, *INHBA*, *TGFBR3*, and *ENG* display clear discrepant profiles of expression among responders and non-responders to both anthracycline and taxane chemotherapy for distinct breast cancer subtypes, specifically luminal A, and serous ovarian cancer. These genes also harbor a possible predictive value to indicate responsiveness to these therapy regimens. Moreover, *ENG* expression could also differentiate luminal A and *HER2*⁺ breast cancers response to taxane therapy. *INHBB* on the other hand had no predictive value in the assessed cancer types.

Gene signatures from inhibins can predict patient survival outcomes

INHA, *TGFBR3*, and *ENG* impact patient outcomes more broadly and more significantly than *INHBB* and *INHBA*. There is also direct functional dependency of *TGFBR3* and *ENG* to inhibin rather than activin [38, 132]. We thus examined signatures associated with either a negative or positive outcome for each of the three genes. Cancer types that presented different survival predictions for *INHA*, *TGFBR3*, or *ENG* were assessed (Fig 5a), and cancer types in which each gene would have a similar patient outcome (i.e., positive overall survival outcome vs. negative overall survival outcome) were separated into groups (e.g., *INHA* positive outcome vs. negative outcome, Fig 5a).

Spearman's ρ coefficient was calculated for all RNA-seq gene data provided in each of these datasets, and values were clustered, and genes that were either positively and negatively correlated with each individual *INHA*, *TGFBR3* or *ENG* genes were identified (S4 Table). The top correlated genes from the positive outcome set were then pairwise compared to genes that had lower correlations in the negative outcome set, and vice-versa to obtain a subset of common genes [133–136]. Examples include *TGFB2* and *HOXA1* where genes correlated to *INHA* in the negative outcome set, and *OGG1* and *STAP2* in the positive outcome group. For *TGFBR3*, *AP1M1* and *RILPL1* correlated in the negative outcome context, while *FZD5* and *MYCN* in the positive one. No gene signatures were obtained for *ENG*. As indicated in section 3.2, the HR value range was the smallest for *ENG* in the assessed cancer types, which limits the differential gene signature analysis. All these genes also had their mRNA expression assessed in the respective cancer sets, contrasted, and evaluated for difference in expression (Fig 5b). Except for 22 genes from sets in which *INHA* or *TGFBR3* had distinct predictions of survival (e.g., *CHSY1*, *LDLR*, *PPARG*, *MIA2*, *TOX3*) all others exhibited significant alterations in gene expression (Fig 5b).

The altered genes from Fig 5b whose difference in expression was significant, were assessed for protein interactions and these iterated for pathway analysis using BioGRID (thebiogrid.org, Fig 5c) [111]. We find that *INHA* gene sets were associated with either *PD-L1* expression and PD-1 checkpoint, Rap1 signaling pathways in patients with positive outcomes or cell cycle

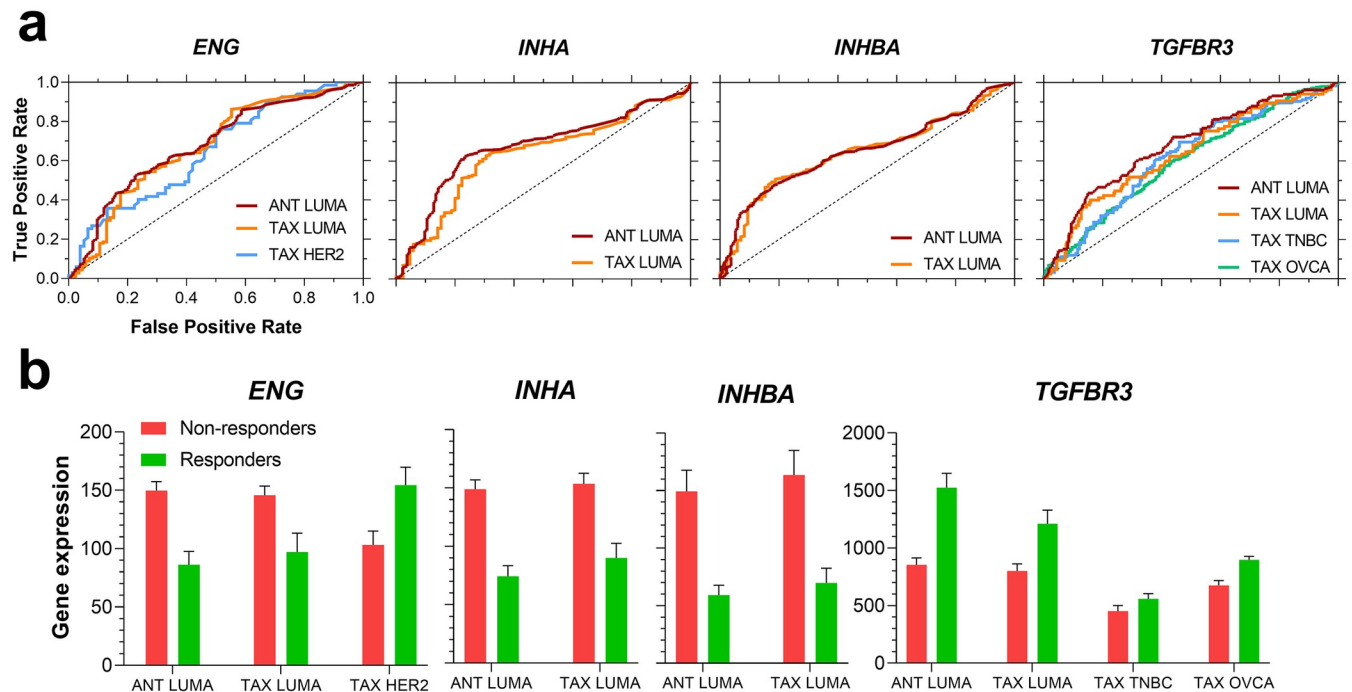


Fig 4. ROC plots (a) and gene expression (b) of indicated genes for different chemotherapy regimens. (a) ROC curves, in which performance ability was verified (i.e., AUC > 0.6), were plotted for *ENG*, *INHA*, *INHBA*, and *TGFBR3*. (b) Gene expression for each investigated gene between responders and non-responders for the assessed pharmacological treatments. The sample sizes for each group were the following: ANT LUMA, n = 474; TAX LUMA, n = 375; TAX HER2, n = 143; TAX TNBC, n = 290; TAX OVCA, n = 851. Abbreviations: ANT: anthracycline; TAX: taxane; LUMA: luminal A; TNBC: triple-negative breast cancer; OVCA: serous ovarian cancer.

<https://doi.org/10.1371/journal.pone.0249558.g004>

regulation in patients with negative outcomes. *TGFBR3* associated genes on the other hand, relied on *VEGF* and *MAPK* signaling pathways for patients with positive outcome and *IL-17*, *p53*, or even *Wnt* signaling pathways in the negative outcome scenario. Detailed descriptions of analyzed genes and pathways are compiled in [S4 Table](#).

To determine if the genes associated with *INHA* and *TGFBR3* had true prognostic value, a Probit regression model was applied to the normalized mRNA expression of the genes in [S5 Table](#). The regressions were analyzed for the cancers from [Fig 2a and 2d](#) which had clear outcomes for either *INHA*, or *TGFBR3*. The final coefficients and entry genes are also provided in [S5 Table](#). We find that the *INHA* model had 43 genes as dependent elements, and the *TGFBR3* model had 37 genes. However, the most suitable model obtained from these sets is the *TGFBR3* model, which has a high goodness of fit p-value ($p = 0.9494$), sensitivity (98.42%), specificity (91.56%), and accuracy (96.70%, [Table 2](#)).

These analyses reveal that a differential signature obtained from *INHA*, along with one of its main binding receptors (i.e., *TGFBR3*) are able to faithfully predict a patient's outcomes in a wide spectrum of cancer types (e.g., kidney, lung, head and neck, breast, liver, ovarian, stomach, endometrial).

Functional analysis and interpretation of inhibin's mechanism of action

Prior functional studies indicate a dependency on *ENG* and *TGFBR3* for inhibin responsiveness [38, 132]. To test if these biological observations hold in patient datasets, we performed supervised clustering using Euclidean algorithm of genes correlating with either *INHA*, *ENG* or *TGFBR3* using the RNA-seq data for cancer types with the most significant impact as

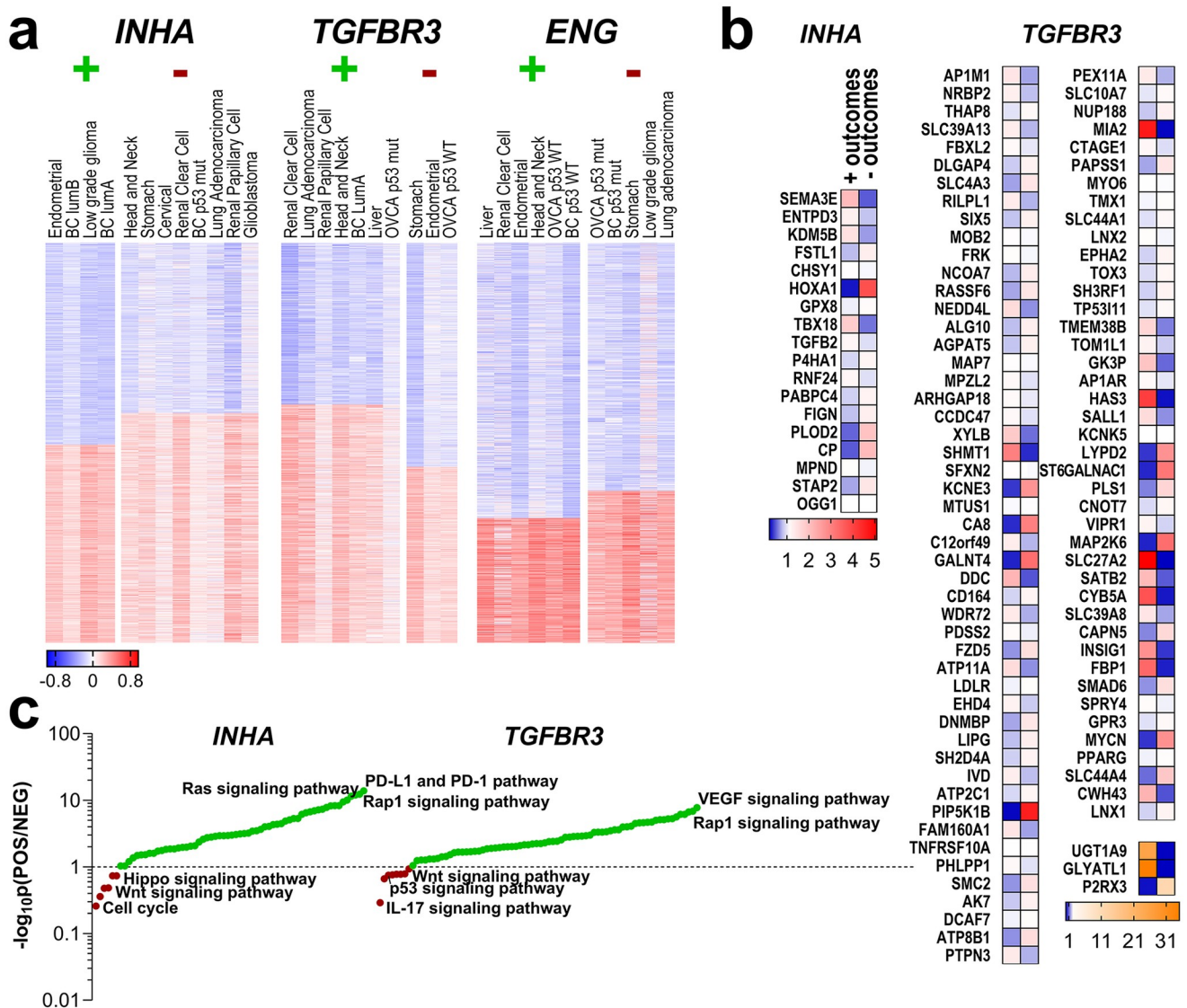


Fig 5. Gene signatures and expression patterns for cancers where *INHA*, *TGFBR3*, or *ENG* predicted survival outcomes. (a) Cancer types in which either *INHA* *TGFBR3* or *ENG* had either positive (+) or negative (-) survival outcomes had their RNA-seq gene data correlation clustered for either low or high degree of correlations to each *INHA*, *TGFBR3* or *ENG* as indicated. (b) mRNA abundance of a subset of common genes obtained from pairwise comparisons of the top correlated genes from the positive outcome with the genes that had lower correlations in the negative outcome set, and vice-versa. mRNA expression was assessed in each cancer set. * $p < 0.05$ ** $p < 0.01$ *** $p < 0.001$ **** $p < 0.0001$ (c) Pathway analysis after BioGRID assessment of the significant genes from (b), ranked with a ratio of significance between sets from the positive and negative outcomes for each gene.

<https://doi.org/10.1371/journal.pone.0249558.g005>

determined in Fig 6a. Only the most enriched transcripts that were either positively or negatively correlated transcripts are shown in Fig 6a. Most enriched genes from these clusters were then compared amongst each other in all pairwise combinations for similarities (e.g., positively correlated to *INHA* vs. negatively correlated to *TGFBR3*, and so on, Fig 6b).

We find that *INHA* and *TGFBR3* comparison rendered 1,430 genes, in which 24.6% were exclusive to *INHA* (e.g., *DLL3*, *GPC2*, *TAZ*, *TERT*, *XYLT2*) 37.7% to *TGFBR3* (e.g., *CCL2*, *CCR4*, *EGFR*, *GLCE*, *IL10RA*, *IL7R*, *ITGA1*, *ITGA2*, *JAK1*, *JAK2*, *SRGN*, *SULF1*, *TGFBR2*), and 13.1% were positively correlated to both (e.g., *CSPG4*, *COL4A3*, *FGF18*, *NOTCH4*, *SMAD9*). When *INHA* was assessed with respect to *ENG* we find 1,773 genes of which, 11.2% were

Table 2. Prognostic performance of each delineated probit model.

	<i>INHA</i> model	<i>TGFBR3</i> model
Cancer types (+)	<ul style="list-style-type: none"> • Endometrial; • BC lum A; • BC lum B; • Low grade glioma 	<ul style="list-style-type: none"> • Renal Clear Cell; • Lung adenocarcinoma; • Renal Papillary Cell; • Head and Neck; • BC lum A; • Liver; • OVCA p53 mut
Cancer types (-)	<ul style="list-style-type: none"> • Head and Neck; • Stomach; • Cervical; • Renal Clear Cell; • BC p53 mut; • Lung adenocarcinoma; • Renal Papillary Cell; • Glioblastoma. 	<ul style="list-style-type: none"> • Stomach; • Endometrial; • OVCA p53 WT.
Genes in model	43	37
Specificity	90.76%	98.42%
Sensitivity	93.17%	91.56%
False positives ratio	6.83%	8.44%
False negative ratio	9.24%	1.58%
Accuracy	92.25%	96.70%

For either an *INHA* or *TGFBR3* model, the described cancer types and subtypes used to analyze the positive (+), and negative (-) outcomes are shown. The number of genes in each model, the model's specificity (i.e., how the model certifies true positives), sensitivity (i.e., how the model certifies true negatives), and their false positive and false negative ratios are shown. The correct classification ratio is also highlighted below.

<https://doi.org/10.1371/journal.pone.0249558.t002>

exclusive to *INHA* (e.g., *GDF9*, *PVT1*), 21.3% to *ENG* (e.g., *CCL2*, *GPC6*, *IL10*, *IL10RA*, *IL7R*, *INHBA*, *ITGA1*, *ITGB2*, *JAK1*, *SRGN*, *SULF1*, *TGFB1*, *TGFBR2*) and 10.0% were highly correlated to both (e.g., *CSPG4*, *DLL1*, *FGF18*, *FZD2*, *NOTCH4*). Lastly, the comparison between *ENG* and *TGFBR3* returned 1,938 genes. However, very few were exclusive to either *TGFBR3* (2.84%) or *ENG* (0.16%), revealing a high functional resemblance between both of these receptors, as most of the profiled genes correlated to both of them (48.5%, e.g., *ADAM9*, -23, *ADAMTS1*, -2, -5, -8, -9, *CCL2*, *CSF1R*, *DLL4*, *ESR1*, *FGF1*, *FGF2*, *FGF18*, *GLI1*, -2, -3, *GPC6*, *IL10RA*, *ITGA1*, *ITGA5*, *JAK1*, *MMP2*, *SDC3*, *SRGN*, *SULF1*, *TGFB3*, *TGFBR2*, *TNC*, *TWIST2*, *XYLT1*, *ZEB1*) or none of them.

We next used each gene set from the cross-comparisons in Fig 6b to identify pathways using KEGG [137]. Unique pathways with an FDR below 5% were identified for the comparisons and are presented in Fig 6c. Although several common pathways were present between groups, such as PI3K-Akt and Ras signaling pathways (see S6 Table), some unique pathways were present as well. *ENG*, for instance, was more exclusively related to cytokine-cytokine receptor interaction and natural killer mediated cytotoxicity (Fig 6c), while *TGFBR3* was more exclusively related to proteoglycans interaction and chemokine signaling. While cell cycle and DNA replication were not directly associated with *ENG* and *TGFBR3*, Rap1 signaling and Extracellular matrix (ECM)-receptor interactions were both impacted by *ENG* and *TGFBR3* (Fig 6c). However, no independent pathway could be pinpointed to *INHA* alone, revealing dependency on either *TGFBR3* or *ENG*. These studies indicate that inhibin's effects may vary

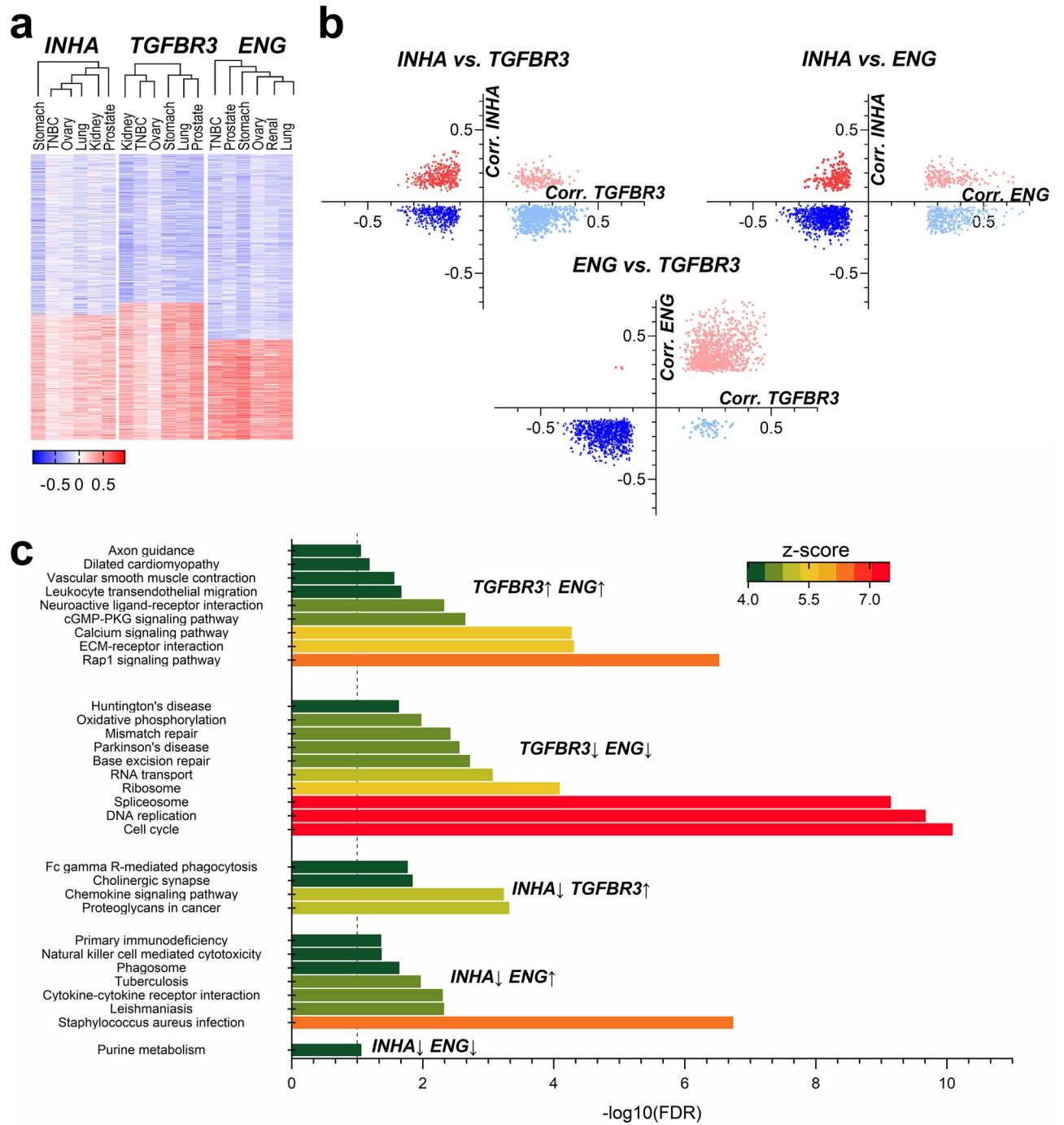


Fig 6. Functional analysis of gene signatures between *INHA* and *TGFBR3* and *INHA* and *ENG*. (a) Supervised clustering of correlations of RNA-seq data between *INHA*, *TGFBR3*, and *ENG* was performed to obtain sets of positive and negatively correlated genes for each set. (b) Common genes that were found in each group of correlated genes (e.g., negative correlation to *INHA* vs. positive to *TGFBR3* and all combinations) is presented. (c) KEGG pathway analysis for groups of genes correlated with the indicated combination. Unique pathways with an FDR below 0.05 were identified for the comparisons and are presented.

<https://doi.org/10.1371/journal.pone.0249558.g006>

depending on whether *ENG* is more highly expressed as compared to *TGFBR3* with significant relevance to defining mechanism and impact of changes in components of this pathway.

Discussion

This study aimed to evaluate comprehensively the influence of the inhibin-activin network in cancer. Our findings provide significant new information on the specific cancers impacted by the genes investigated here, *INHA*, *INHBA*, *INHBB*, *ENG* and *TGFFBR3*, and shed light on potential functional dependencies. Additional gene signature analysis reveals that *INHA*, along with one of its main receptors (i.e., *TGBFR3*) faithfully predicts patient outcomes in a wide spectrum of cancer types.

TGF β -1 is a representative member of the TGF- β family that has been significantly investigated previously [138]. However, less information exists about the precise impact and role of other members like inhibins and activins. Our findings that *INHA* is significantly associated with survival in sixteen of the twenty cancers analyzed, correlating positively with survival in five cancers and negatively in ten (Fig 2), highlight *INHA*'s differential role as a tumor suppressor or promoter depending on the specific cancer type. In highly angiogenic tumors like renal clear cell carcinoma [139] and glioblastoma [140], we found *INHA* expression to be a significant negative predictor of survival. *INHA*'s role in promoting tumorigenesis in these cancer types may occur through its effects on angiogenesis as has been previously reported for a subset of ovarian and prostate cancer [27, 72] warranting further investigation. In Luminal A breast cancers, we observed that increased *INHA* expression was associated with unresponsiveness to chemotherapy (Fig 4) while in survival data it was a positive predictor of survival (Fig 2). This apparent contradiction can perhaps be explained by the fact that data in KM Plotter contains information on patients that have undergone a wide array of treatments. Likely, *INHA* is predictive of response to some treatments but not others. In both breast and ovarian cancers, *INHA* was a negative predictor of survival in patients that had p53 mutations indicating a potential dependency of *INHA* functions on the p53 status. *INHA* expression alterations have been observed in p53 mutated adrenocortical tumors and *INHA* was suggested to be a contributing factor to tumorigenesis in these cancers [141]. One of the most characterized transcriptional activators of *INHA* is GATA4 [142], which can also regulate p53 in cancer and could contribute to the different survival outcomes observed for *INHA* in p53 mutated cancers versus wild-type p53 cancers [143, 144]. *INHA*'s link to functional outcomes in the background on p53 mutations remains to be fully elucidated.

Between the TGF- β family co-receptors (*ENG* and *TGFBR3*) implicated in cancer progression and inhibin function, *ENG* was more expressed (Fig 1c), particularly in lung adenocarcinoma and gastric cancers, corresponding with *ENG* being a strong negative predictor of survival (Figs 1c and 2). These findings are consistent with prior experimental findings as well [145, 146]. In p53 mutated cancers, *ENG* remained a negative predictor. ROC Plotter analysis revealed decreased *ENG* expression to be associated with response to anthracycline therapy in Luminal A breast cancer patients (Fig 4). However, a previous study showed that positive *ENG* expression was associated with increased survival in breast cancer patients who had undergone anthracycline treatment [147]. While Isacke and colleagues did not report a specific subtype in their analyzed cohort [147], we obtained significant results for Luminal A breast cancer, specifically. Moreover, an additional study performed in acute myeloid leukemia showed an inverse relationship to that of Isacke et al., consistent with our results in Luminal A breast cancer [147, 148]. We also found *ENG* to be a predictive of response to taxane therapy regimens. An inverse relationship between *ENG* expression was observed in responders for Luminal A and *HER2*⁺ breast cancer, with responders expressing high *ENG* in *HER2*⁺ breast cancers but low levels of

ENG in Luminal A cancers (Fig 4). As Luminal A breast cancer is *HER2*⁻, *ENG* could be affected by *HER2* status in these cancer types. In our analysis, expression data was only obtained for Luminal A breast cancers not *HER2*⁺ so differences in expression between the two were not analyzed.

Consistent with *TGFBR3*'s role as a tumor suppressor in many cancers, we found it to be a significant positive predictor of survival in all but two cancers (i.e., endometrial and all gastric subtypes, Fig 2). Increased *TGFBR3* was predictive of response in all treatments and cancers we examined (Fig 4), further bolstering *TGFBR3*'s role as a negative regulator of tumor progression. Specifically, Bholra et al. (2013) [149] showed increased levels of *TGFBR3* in response to taxane in a small cohort (n = 17) of breast cancer patients; however, response to therapy was not analyzed. *TGFBR3* has been shown to act as a tumor suppressor in renal clear cell carcinoma [127] and non-small cell lung cancers [102] which was also confirmed here (Fig 2). We were also able to expand *TGFBR3*'s role in renal cancer to papillary carcinomas as well (Fig 2).

Expression of *ENG* and *TGFBR3* was not significantly different between wild-type and p53 mutated cancers indicating p53 likely does not impact expression itself. Whether protein secretion of these coreceptors is altered in these cancers is currently unknown, and cannot be ruled out, as previous studies have shown increased endoglin folding and maturation in p53 mutation settings [150]. *TGFBR3* also undergoes N-linked glycosylation, so a similar scenario to endoglin is possible. Alterations in protein maturation could explain the differential patient outcomes observed between wild-type and p53 mutated cancers, when assessing for *ENG* and *TGFBR3*, despite changes in expression not being observed.

INHA's dependency on each coreceptor examined in survival analysis revealed distinct signatures between different cancer types (Table 1). Prior studies indicate a requirement for *ENG* in inhibin responsiveness and functions [27], which was borne out in patient survival data here (Table 1). However, a few outliers exist such as p53 mutated breast and renal clear cell carcinoma where *INHA* was not always dependent on increased *ENG* and *TGFBR3* expression. We found *INHA* to only be a negative predictor of survival in patients expressing low *ENG* indicating *INHA* might act independent of either coreceptor in these cancer types. The role of other receptors involved in mediating *INHA*'s effects in these cancer types remains to be determined.

Betaglycan and endoglin are co-receptors for TGF β -1,2,3 and have been shown to regulate signaling for isoforms of BMP, Wnt and FGF [151–153]. However, both endoglin and betaglycan are dispensable for response to the above-mentioned growth factors, playing primarily modulatory functions. Given that TGF- β 's BMPs, Wnt, and FGF can act as both tumor suppressors and promoters in a cancer and context dependent manner, and our analysis indicating that *ENG* and *TGFBR3* are both strong predictors of survival on their own (Fig 2) it is likely that *ENG* and *TGFBR3* expression levels impact signaling sensitivity and thereby patient outcomes in the context of those signaling ligands.

In contrast to the above listed growth factors, Inhibins are reported to have functional consequences that dependent primarily on betaglycan or endoglin [23, 27] consistent with the ability of the gene signatures (Fig 5) dependent on *TGFBR3* and *ENG* to distinguish patients' outcomes. Some notable elements of this signature have been verified previously and even proposed as cancer biomarkers. For example, *EPHA2* overexpression has been associated with decreased patient survival and promotes drug resistance, increased invasion, and epithelial to mesenchymal transition (EMT) [154–157]. *HOXA1*, a lncRNA overexpressed in cancers such as breast, melanoma, and oral carcinomas, drives metastasis and tamoxifen resistance [158–160]. For *TGFBR3* specifically, three genes revealed high discrimination between positive and negative outcomes: *UGT1A9* and *GLYATL1* were 25- and 35-fold more expressed in positive outcomes and *P2RX3* was 11.5-fold more expressed in negative outcomes. Of interest,

UGT1A9 is a UDP-glucuronosyltransferase (UGT) whose activity has been implicated in drug resistance by affecting the bioactivity of the drug [161, 162]. We speculate that as a proteoglycan, increased *TGFBR3* could compete for UDP-glucuronate acid (GlcA) and UDP-xylose, both key elements for UGT1A9 activity, thereby potentially disrupting UGT associated resistance mechanisms and increasing the efficacy of chemotherapy. We also narrowed down which pathways differentiated patient outcomes for either *INHA* or *TGFBR3*. For positive outcomes, we found that *INHA* was associated with PD-L1, Ras, and Rap1 signaling pathways. In adverse outcomes, *INHA* was associated with Hippo, Wnt, and cell cycle pathways. Wnt has been shown to regulate *INHA* transcription in rat adrenal cortex and could increase *INHA* expression in certain tumors to promote tumorigenesis [163]. Recent evidence indicates increased PD-L1 in dendritic cells in *INHA*^{-/-} mice [164]. We speculate that increased *INHA* in tumors may inhibit PD-L1 expression perhaps via antagonistic effect on other TGF- β members, increasing anti-tumor immune responses.

There are currently no other cancer prognostic models based on our three assessed genes. The selected prognostic model showed high accuracy (96.7%) with 98.42% sensitivity and 91.56% specificity (Table 2). Moreover, most prognostic cancer models are directed to either a specific cancer type (e.g., breast, prostate) or a cancer stage (e.g., lymph node metastases, phases). Our model includes at least ten tumor types, is in the top two for sensitivity, and among the second quartile of specificities on assessment of 48 prognostic cancer models [165–168]. Thus, the *INHA-TGFBR3-ENG* signature has pan-cancer prognostic value. Interestingly, there were very few SMAD and canonical TGF- β associated pathway members that were part of the probit analysis (S5 Table). However, several genes associated with non-SMAD TGF- β signaling were included, such as *MAP2K6*, *FZD5*, and *PHLPP1* which are associated with MAPK, Wnt, and Akt signaling pathways respectively [169]. Much of TGF- β 's functions in EMT, invasion and metastasis have been associated with non-SMAD pathways [169, 170] which are more likely to involve the coreceptors *TGFBR3* and *ENG*. Hence it was not surprising that such non SMAD pathways were predominant in the *INHA-TGFBR3-ENG* analysis.

Clustering analysis for genes correlated with *INHA*, *TGFBR3*, or *ENG* in cancers (Fig 6) revealed *ENG* and *TGFBR3* had very few genes correlated exclusively to one or the other. As both receptors share similar structures and interact with common ligands [38], this is not unexpected. Similarly, since *ENG* and *TGFBR3* had significant common gene associations this resulted in common pathways. For instance, a strong correlation with ECM-receptors and Rap1 signaling was observed. *ENG* has been shown to bind leukocyte integrins, promoting invasion [171], and ECM remodeling during fibrosis [172]. *TGFBR3* has been shown to regulate integrin localization and adhesion to ECM [173]. *ENG* alone was associated with natural killer cell-mediated cytotoxicity consistent with previous findings showing anti-endoglin therapy augmented immune response in tumors by increasing NK cells, CD4⁺, and CD8⁺ T lymphocytes [174].

In conclusion, our pan-cancer analysis of the inhibin-activin network reveals a prognostic signature capable of accurately predicting patient outcome. Gene signatures from our analysis reveal robust relationships between *INHA*, *ENG*, and *TGFBR3* and other established cancer biomarkers. Survival analysis implicated members of the inhibin-activin network in cancers previously unstudied as well as corroborated previous findings. Further analysis of the role of the inhibin-activin network in cancer and relationship to other cancer associated genes, as well as validation as predictive biomarkers to chemotherapy is needed.

Supporting information

S1 Table. Supplementary data regarding gene expression, alteration and dependency. (XLSX)

S2 Table. Complementary table for survival data.
(DOCX)

S3 Table. Full data concerning ROC analysis.
(XLSX)

S4 Table. INHA, TGFBR3 and ENG survival gene signature full data discrimination.
(XLSB)

S5 Table. Probit regression detailed outputs.
(XLSX)

S6 Table. INHA-TGFBR3-ENG pairwise gene comparison data.
(XLSX)

Author Contributions

Conceptualization: Eduardo Listik, Ben Horst, Nam. Y. Lee, Karthikeyan Mythreya.

Formal analysis: Eduardo Listik, Ben Horst, Alex Seok Choi, Karthikeyan Mythreya.

Funding acquisition: Karthikeyan Mythreya.

Investigation: Ben Horst, Karthikeyan Mythreya.

Methodology: Eduardo Listik, Ben Horst, Balázs Györfy, Karthikeyan Mythreya.

Supervision: Karthikeyan Mythreya.

Validation: Eduardo Listik, Balázs Györfy.

Visualization: Eduardo Listik, Ben Horst, Alex Seok Choi, Karthikeyan Mythreya.

Writing – original draft: Eduardo Listik, Ben Horst, Karthikeyan Mythreya.

Writing – review & editing: Eduardo Listik, Ben Horst, Alex Seok Choi, Nam. Y. Lee, Balázs Györfy, Karthikeyan Mythreya.

References

1. Schwartz NB, Channing CP. Evidence for ovarian "inhibin": suppression of the secondary rise in serum follicle stimulating hormone levels in proestrous rats by injection of porcine follicular fluid. *Proc Natl Acad Sci U S A*. 1977; 74(12):5721–4. <https://doi.org/10.1073/pnas.74.12.5721> PMID: 271996.
2. Keogh EJ, Lee VW, Rennie GC, Burger HG, Hudson B, De Kretser DM. Selective suppression of FSH by testicular extracts. *Endocrinology*. 1976; 98(4):997–1004. <https://doi.org/10.1210/endo-98-4-997> PMID: 1278104.
3. De Jong FH, Sharpe RM. Evidence for inhibin-like activity in bovine follicular fluid. *Nature*. 1976; 263(5572):71–2. <https://doi.org/10.1038/263071a0> PMID: 958466.
4. Setchell BP, Jacks F. Inhibin-like activity in rete testis fluid. *J Endocrinol*. 1974; 62(3):675–6. <https://doi.org/10.1677/joe.0.0620675> PMID: 4413885.
5. Woodruff TK, Lyon RJ, Hansen SE, Rice GC, Mather JP. Inhibin and activin locally regulate rat ovarian folliculogenesis. *Endocrinology*. 1990; 127(6):3196–205. <https://doi.org/10.1210/endo-127-6-3196> PMID: 2123449.
6. Cate RL, Mattaliano RJ, Hession C, Tizard R, Farber NM, Cheung A, et al. Isolation of the bovine and human genes for Müllerian inhibiting substance and expression of the human gene in animal cells. *Cell*. 1986; 45(5):685–98. [https://doi.org/10.1016/0092-8674\(86\)90783-x](https://doi.org/10.1016/0092-8674(86)90783-x) PMID: 3754790.
7. Gaddy-Kurten D, Vale WW. Activin increases phosphorylation and decreases stability of the transcription factor Pit-1 in MtTW15 somatotrope cells. *J Biol Chem*. 1995; 270(48):28733–9. <https://doi.org/10.1074/jbc.270.48.28733> PMID: 7499395.

8. Makanji Y, Zhu J, Mishra R, Holmquist C, Wong WP, Schwartz NB, et al. Inhibin at 90: from discovery to clinical application, a historical review. *Endocr Rev.* 2014; 35(5):747–94. Epub 2014/07/22. <https://doi.org/10.1210/er.2014-1003> PMID: 25051334.
9. Ling N, Ying SY, Ueno N, Shimasaki S, Esch F, Hotta M, et al. A homodimer of the beta-subunits of inhibin A stimulates the secretion of pituitary follicle stimulating hormone. *Biochem Biophys Res Commun.* 1986; 138(3):1129–37. [https://doi.org/10.1016/s0006-291x\(86\)80400-4](https://doi.org/10.1016/s0006-291x(86)80400-4) PMID: 3092817.
10. Vale W, Rivier J, Vaughan J, McClintock R, Corrigan A, Woo W, et al. Purification and characterization of an FSH releasing protein from porcine ovarian follicular fluid. *Nature.* 1986; 321(6072):776–9. <https://doi.org/10.1038/321776a0> PMID: 3012369.
11. W V, A H, C R, J Y. The Inhibin/Activin Family of Hormones and Growth Factors. Peptide Growth Factors and Their Receptors II. 95. *Handbook of Experimental Pharmacology*: Springer, Berlin, Heidelberg; 1990.
12. Antenos M, Zhu J, Jetly NM, Woodruff TK. An activin/furin regulatory loop modulates the processing and secretion of inhibin alpha- and betaB-subunit dimers in pituitary gonadotrope cells. *J Biol Chem.* 2008; 283(48):33059–68. Epub 2008/09/30. <https://doi.org/10.1074/jbc.M804190200> PMID: 18826955.
13. Robertson DM, Foulds LM, Leversha L, Morgan FJ, Hearn MT, Burger HG, et al. Isolation of inhibin from bovine follicular fluid. *Biochem Biophys Res Commun.* 1985; 126(1):220–6. [https://doi.org/10.1016/0006-291x\(85\)90594-7](https://doi.org/10.1016/0006-291x(85)90594-7) PMID: 3918529.
14. Rivier J, Spiess J, McClintock R, Vaughan J, Vale W. Purification and partial characterization of inhibin from porcine follicular fluid. *Biochem Biophys Res Commun.* 1985; 133(1):120–7. [https://doi.org/10.1016/0006-291x\(85\)91849-2](https://doi.org/10.1016/0006-291x(85)91849-2) PMID: 4074357.
15. Ueno N, Ling N, Ying SY, Esch F, Shimasaki S, Guillemin R. Isolation and partial characterization of follistatin: a single-chain Mr 35,000 monomeric protein that inhibits the release of follicle-stimulating hormone. *Proc Natl Acad Sci U S A.* 1987; 84(23):8282–6. <https://doi.org/10.1073/pnas.84.23.8282> PMID: 3120188.
16. Miyamoto K, Hasegawa Y, Fukuda M, Nomura M, Igarashi M, Kangawa K, et al. Isolation of porcine follicular fluid inhibin of 32K daltons. *Biochem Biophys Res Commun.* 1985; 129(2):396–403. [https://doi.org/10.1016/0006-291x\(85\)90164-0](https://doi.org/10.1016/0006-291x(85)90164-0) PMID: 4015638.
17. Attisano L, Wrana JL. Signal transduction by the TGF-beta superfamily. *Science.* 2002; 296(5573):1646–7. <https://doi.org/10.1126/science.1071809> PMID: 12040180.
18. Attisano L, Wrana JL, López-Casillas F, Massagué J. TGF-beta receptors and actions. *Biochim Biophys Acta.* 1994; 1222(1):71–80. [https://doi.org/10.1016/0167-4889\(94\)90026-4](https://doi.org/10.1016/0167-4889(94)90026-4) PMID: 8186268.
19. Gray PC, Greenwald J, Blount AL, Kunitake KS, Donaldson CJ, Choe S, et al. Identification of a binding site on the type II activin receptor for activin and inhibin. *J Biol Chem.* 2000; 275(5):3206–12. <https://doi.org/10.1074/jbc.275.5.3206> PMID: 10652306.
20. Attisano L, Cárcamo J, Ventura F, Weis FM, Massagué J, Wrana JL. Identification of human activin and TGF beta type I receptors that form heteromeric kinase complexes with type II receptors. *Cell.* 1993; 75(4):671–80. [https://doi.org/10.1016/0092-8674\(93\)90488-c](https://doi.org/10.1016/0092-8674(93)90488-c) PMID: 8242742.
21. Ebner R, Chen RH, Lawler S, Zioncheck T, Derynck R. Determination of type I receptor specificity by the type II receptors for TGF-beta or activin. *Science.* 1993; 262(5135):900–2. <https://doi.org/10.1126/science.8235612> PMID: 8235612.
22. Attisano L, Wrana JL, Montalvo E, Massagué J. Activation of signalling by the activin receptor complex. *Mol Cell Biol.* 1996; 16(3):1066–73. <https://doi.org/10.1128/mcb.16.3.1066> PMID: 8622651.
23. Lewis KA, Gray PC, Blount AL, MacConell LA, Wiater E, Bilezikjian LM, et al. Betaglycan binds inhibin and can mediate functional antagonism of activin signalling. *Nature.* 2000; 404(6776):411–4. Epub 2000/04/04. <https://doi.org/10.1038/35006129> PMID: 10746731.
24. Zhu J, Lin SJ, Zou C, Makanji Y, Jardetzky TS, Woodruff TK. Inhibin α -subunit N terminus interacts with activin type IB receptor to disrupt activin signaling. *J Biol Chem.* 2012; 287(11):8060–70. Epub 2012/01/20. <https://doi.org/10.1074/jbc.M111.293381> PMID: 22267736.
25. Chong H, Pangas SA, Bernard DJ, Wang E, Gitich J, Chen W, et al. Structure and expression of a membrane component of the inhibin receptor system. *Endocrinology.* 2000; 141(7):2600–7. <https://doi.org/10.1210/endo.141.7.7540> PMID: 10875264.
26. Chapman SC, Bernard DJ, Jelen J, Woodruff TK. Properties of inhibin binding to betaglycan, InhBP/p120 and the activin type II receptors. *Mol Cell Endocrinol.* 2002; 196(1–2):79–93. [https://doi.org/10.1016/s0303-7207\(02\)00227-7](https://doi.org/10.1016/s0303-7207(02)00227-7) PMID: 12385827.
27. Singh P, Jenkins LM, Horst B, Alers V, Pradhan S, Kaur P, et al. Inhibin Is a Novel Paracrine Factor for Tumor Angiogenesis and Metastasis. *Cancer Res.* 2018; 78(11):2978–89. Epub 2018/03/13. <https://doi.org/10.1158/0008-5472.CAN-17-2316> PMID: 29535220.

28. López-Casillas F, Cheifetz S, Doody J, Andres JL, Lane WS, Massagué J. Structure and expression of the membrane proteoglycan betaglycan, a component of the TGF-beta receptor system. *Cell*. 1991; 67(4):785–95. [https://doi.org/10.1016/0092-8674\(91\)90073-8](https://doi.org/10.1016/0092-8674(91)90073-8) PMID: 1657406.
29. Wang XF, Lin HY, Ng-Eaton E, Downward J, Lodish HF, Weinberg RA. Expression cloning and characterization of the TGF-beta type III receptor. *Cell*. 1991; 67(4):797–805. [https://doi.org/10.1016/0092-8674\(91\)90074-9](https://doi.org/10.1016/0092-8674(91)90074-9) PMID: 1657407.
30. Gougos A, Letarte M. Primary structure of endoglin, an RGD-containing glycoprotein of human endothelial cells. *J Biol Chem*. 1990; 265(15):8361–4. PMID: 1692830.
31. Chen W, Kirkbride KC, How T, Nelson CD, Mo J, Frederick JP, et al. Beta-arrestin 2 mediates endocytosis of type III TGF-beta receptor and down-regulation of its signaling. *Science*. 2003; 301(5638):1394–7. <https://doi.org/10.1126/science.1083195> PMID: 12958365.
32. McLean S, Bhattacharya M, Di Guglielmo GM. β arrestin2 interacts with T β RII to regulate Smad-dependent and Smad-independent signal transduction. *Cell Signal*. 2013; 25(1):319–31. Epub 2012/10/13. <https://doi.org/10.1016/j.cellsig.2012.10.001> PMID: 23069267.
33. Blobel GC, Liu X, Fang SJ, How T, Lodish HF. A novel mechanism for regulating transforming growth factor beta (TGF-beta) signaling. Functional modulation of type III TGF-beta receptor expression through interaction with the PDZ domain protein, GIPC. *J Biol Chem*. 2001; 276(43):39608–17. Epub 2001/08/23. <https://doi.org/10.1074/jbc.M106831200> PMID: 11546783.
34. Myhre K, Blobel GC. The type III TGF-beta receptor regulates epithelial and cancer cell migration through beta-arrestin2-mediated activation of Cdc42. *Proc Natl Acad Sci U S A*. 2009; 106(20):8221–6. Epub 2009/05/07. <https://doi.org/10.1073/pnas.0812879106> PMID: 19416857.
35. Lee NY, Ray B, How T, Blobel GC. Endoglin promotes transforming growth factor beta-mediated Smad 1/5/8 signaling and inhibits endothelial cell migration through its association with GIPC. *J Biol Chem*. 2008; 283(47):32527–33. Epub 2008/09/05. <https://doi.org/10.1074/jbc.M803059200> PMID: 18775991.
36. Lee NY, Blobel GC. The interaction of endoglin with beta-arrestin2 regulates transforming growth factor-beta-mediated ERK activation and migration in endothelial cells. *J Biol Chem*. 2007; 282(29):21507–17. Epub 2007/05/31. <https://doi.org/10.1074/jbc.M700176200> PMID: 17540773.
37. Cheifetz S, Bellón T, Calés C, Vera S, Bernabeu C, Massagué J, et al. Endoglin is a component of the transforming growth factor-beta receptor system in human endothelial cells. *J Biol Chem*. 1992; 267(27):19027–30. PMID: 1326540.
38. Kim SK, Henen MA, Hinck AP. Structural biology of betaglycan and endoglin, membrane-bound co-receptors of the TGF-beta family. *Exp Biol Med* (Maywood). 2019; 244(17):1547–58. Epub 2019/10/10. <https://doi.org/10.1177/1535370219881160> PMID: 31601110.
39. Letamendía A, Lastres P, Botella LM, Raab U, Langa C, Velasco B, et al. Role of endoglin in cellular responses to transforming growth factor-beta. A comparative study with betaglycan. *J Biol Chem*. 1998; 273(49):33011–9. <https://doi.org/10.1074/jbc.273.49.33011> PMID: 9830054.
40. Stenvers KL, Tursky ML, Harder KW, Kountouri N, Amatayakul-Chantler S, Grail D, et al. Heart and liver defects and reduced transforming growth factor beta2 sensitivity in transforming growth factor beta type III receptor-deficient embryos. *Mol Cell Biol*. 2003; 23(12):4371–85. <https://doi.org/10.1128/mcb.23.12.4371-4385.2003> PMID: 12773577.
41. Compton LA, Potash DA, Brown CB, Barnett JV. Coronary vessel development is dependent on the type III transforming growth factor beta receptor. *Circ Res*. 2007; 101(8):784–91. Epub 2007/08/17. <https://doi.org/10.1161/CIRCRESAHA.107.152082> PMID: 17704211.
42. Li DY, Sorensen LK, Brooke BS, Urness LD, Davis EC, Taylor DG, et al. Defective angiogenesis in mice lacking endoglin. *Science*. 1999; 284(5419):1534–7. <https://doi.org/10.1126/science.284.5419.1534> PMID: 10348742.
43. Arthur HM, Ure J, Smith AJ, Renforth G, Wilson DI, Torsney E, et al. Endoglin, an ancillary TGFbeta receptor, is required for extraembryonic angiogenesis and plays a key role in heart development. *Dev Biol*. 2000; 217(1):42–53. <https://doi.org/10.1006/dbio.1999.9534> PMID: 10625534.
44. López-Novoa JM, Bernabeu C. The physiological role of endoglin in the cardiovascular system. *Am J Physiol Heart Circ Physiol*. 2010; 299(4):H959–74. Epub 2010/07/23. <https://doi.org/10.1152/ajpheart.01251.2009> PMID: 20656886.
45. Miller DW, Graulich W, Karges B, Stahl S, Ernst M, Ramaswamy A, et al. Elevated expression of endoglin, a component of the TGF-beta-receptor complex, correlates with proliferation of tumor endothelial cells. *Int J Cancer*. 1999; 81(4):568–72. [https://doi.org/10.1002/\(sici\)1097-0215\(19990517\)81:4<568::aid-ijc11>3.0.co;2-x](https://doi.org/10.1002/(sici)1097-0215(19990517)81:4<568::aid-ijc11>3.0.co;2-x) PMID: 10225446.
46. Jenkins LM, Horst B, Lancaster CL, Myhre K. Dually modified transmembrane proteoglycans in development and disease. *Cytokine Growth Factor Rev*. 2018; 39:124–36. Epub 2018/01/03. <https://doi.org/10.1016/j.cytogr.2017.12.003> PMID: 29291930.

47. Mythreya K, Blobel GC. Proteoglycan signaling co-receptors: roles in cell adhesion, migration and invasion. *Cell Signal*. 2009; 21(11):1548–58. Epub 2009/05/08. <https://doi.org/10.1016/j.cellsig.2009.05.001> PMID: 19427900.
48. Gatza CE, Holtzhausen A, Kirkbride KC, Morton A, Gatza ML, Datto MB, et al. Type III TGF- β receptor enhances colon cancer cell migration and anchorage-independent growth. *Neoplasia*. 2011; 13(8):758–70. <https://doi.org/10.1593/neo.11528> PMID: 21847367.
49. Burrows FJ, Derbyshire EJ, Tazzari PL, Amlot P, Gazdar AF, King SW, et al. Up-regulation of endoglin on vascular endothelial cells in human solid tumors: implications for diagnosis and therapy. *Clin Cancer Res*. 1995; 1(12):1623–34. PMID: 9815965.
50. Paauwe M, Heijkants RC, Oudt CH, van Pelt GW, Cui C, Theuer CP, et al. Endoglin targeting inhibits tumor angiogenesis and metastatic spread in breast cancer. *Oncogene*. 2016; 35(31):4069–79. Epub 2016/01/25. <https://doi.org/10.1038/onc.2015.509> PMID: 26804178.
51. Oxmann D, Held-Feindt J, Stark AM, Hattermann K, Yoneda T, Mentlein R. Endoglin expression in metastatic breast cancer cells enhances their invasive phenotype. *Oncogene*. 2008; 27(25):3567–75. Epub 2008/01/28. <https://doi.org/10.1038/sj.onc.1211025> PMID: 18223685.
52. Paauwe M, Schoonderwoerd MJA, Helderma R, Harryvan TJ, Groenewoud A, van Pelt GW, et al. Endoglin Expression on Cancer-Associated Fibroblasts Regulates Invasion and Stimulates Colorectal Cancer Metastasis. *Clin Cancer Res*. 2018; 24(24):6331–44. Epub 2018/06/26. <https://doi.org/10.1158/1078-0432.CCR-18-0329> PMID: 29945992.
53. Hempel N, How T, Dong M, Murphy SK, Fields TA, Blobel GC. Loss of betaglycan expression in ovarian cancer: role in motility and invasion. *Cancer Res*. 2007; 67(11):5231–8. Epub 2007/05/23. <https://doi.org/10.1158/0008-5472.CAN-07-0035> PMID: 17522389.
54. Gordon KJ, Dong M, Chislock EM, Fields TA, Blobel GC. Loss of type III transforming growth factor beta receptor expression increases motility and invasiveness associated with epithelial to mesenchymal transition during pancreatic cancer progression. *Carcinogenesis*. 2008; 29(2):252–62. Epub 2007/11/13. <https://doi.org/10.1093/carcin/bgm249> PMID: 17999987.
55. Turley RS, Finger EC, Hempel N, How T, Fields TA, Blobel GC. The type III transforming growth factor-beta receptor as a novel tumor suppressor gene in prostate cancer. *Cancer Res*. 2007; 67(3):1090–8. <https://doi.org/10.1158/0008-5472.CAN-06-3117> PMID: 17283142.
56. Cook LM, Frieling JS, Nerlakanti N, McGuire JJ, Stewart PA, Burger KL, et al. Betaglycan drives the mesenchymal stromal cell osteogenic program and prostate cancer-induced osteogenesis. *Oncogene*. 2019; 38(44):6959–69. Epub 2019/08/13. <https://doi.org/10.1038/s41388-019-0913-4> PMID: 31409900.
57. Jovanović B, Beeler JS, Pickup MW, Chytil A, Gorska AE, Ashby WJ, et al. Transforming growth factor beta receptor type III is a tumor promoter in mesenchymal-stem like triple negative breast cancer. *Breast Cancer Res*. 2014; 16(4):R69. Epub 2014/07/01. <https://doi.org/10.1186/bcr3684> PMID: 24985072.
58. Woszczyk D, Gola J, Jurzak M, Mazurek U, Mykała-Cieśla J, Wilczok T. Expression of TGF beta 1 genes and their receptor types I, II, and III in low- and high-grade malignancy non-Hodgkin's lymphomas. *Med Sci Monit*. 2004; 10(1):CR33–7. PMID: 14704634.
59. Zhang J, Zhang L, Lin Q, Ren W, Xu G. Prognostic value of endoglin-assessed microvessel density in cancer patients: a systematic review and meta-analysis. *Oncotarget*. 2018; 9(7):7660–71. Epub 2017/12/21. <https://doi.org/10.18632/oncotarget.23546> PMID: 29484142.
60. Bai S, Zhu W, Coffman L, Vlad A, Schwartz LE, Elishaev E, et al. CD105 Is Expressed in Ovarian Cancer Precursor Lesions and Is Required for Metastasis to the Ovary. *Cancers (Basel)*. 2019; 11(11). Epub 2019/11/02. <https://doi.org/10.3390/cancers11111710> PMID: 31684072.
61. Zhang J, Yuan B, Zhang H, Li H. Human epithelial ovarian cancer cells expressing CD105, CD44 and CD106 surface markers exhibit increased invasive capacity and drug resistance. *Oncol Lett*. 2019; 17(6):5351–60. Epub 2019/04/05. <https://doi.org/10.3892/ol.2019.10221> PMID: 31186752.
62. Matzuk MM, Finegold MJ, Su JG, Hsueh AJ, Bradley A. Alpha-inhibin is a tumour-suppressor gene with gonadal specificity in mice. *Nature*. 1992; 360(6402):313–9. <https://doi.org/10.1038/360313a0> PMID: 1448148.
63. Shanbhag SA, Sheth AR, Nanivadekar SA, Sheth NA. Immunoreactive inhibin-like material in serum and gastric juice of patients with benign and malignant diseases of the stomach. *Br J Cancer*. 1985; 51(6):877–82. <https://doi.org/10.1038/bjc.1985.133> PMID: 4005143.
64. Suzuki Y, Sugiyama M, Abe N, Fujioka Y, Atomi Y. Immunohistochemical similarities between pancreatic mucinous cystic tumor and ovarian mucinous cystic tumor. *Pancreas*. 2008; 36(1):e40–6. <https://doi.org/10.1097/mpa.0b013e3181584643> PMID: 18192871.

65. McCluggage WG, Maxwell P, Patterson A, Sloan JM. Immunohistochemical staining of hepatocellular carcinoma with monoclonal antibody against inhibin. *Histopathology*. 1997; 30(6):518–22. <https://doi.org/10.1046/j.1365-2559.1997.5580774.x> PMID: 9205855.
66. Arora DS, Cooke IE, Ganesan TS, Ramsdale J, Manek S, Charnock FM, et al. Immunohistochemical expression of inhibin/activin subunits in epithelial and granulosa cell tumours of the ovary. *J Pathol*. 1997; 181(4):413–8. [https://doi.org/10.1002/\(SICI\)1096-9896\(199704\)181:4<413::AID-PATH789>3.0.CO;2-U](https://doi.org/10.1002/(SICI)1096-9896(199704)181:4<413::AID-PATH789>3.0.CO;2-U) PMID: 9196439.
67. Huang JJ, Blobe GC. Dichotomous roles of TGF- β in human cancer. *Biochem Soc Trans*. 2016; 44(5):1441–54. <https://doi.org/10.1042/BST20160065> PMID: 27911726.
68. Ball EM, Mellor SL, Risbridger GP. Cancer progression: is inhibin alpha from Venus or Mars? *Cytokine Growth Factor Rev*. 2004; 15(5):291–6. <https://doi.org/10.1016/j.cytogfr.2004.04.004> PMID: 15450247.
69. Risbridger GP, Ball EM, Wang H, Mellor SL, Peehl DM. Re-evaluation of inhibin alpha subunit as a tumour suppressor in prostate cancer. *Mol Cell Endocrinol*. 2004; 225(1–2):73–6. <https://doi.org/10.1016/j.mce.2004.02.015> PMID: 15451570.
70. Robertson DM, Pruyers E, Jobling T. Inhibin as a diagnostic marker for ovarian cancer. *Cancer Lett*. 2007; 249(1):14–7. Epub 2007/02/22. <https://doi.org/10.1016/j.canlet.2006.12.017> PMID: 17320281.
71. Walentowicz P, Krintus M, Sadlecki P, Grabiec M, Mankowska-Cyl A, Sokup A, et al. Serum inhibin A and inhibin B levels in epithelial ovarian cancer patients. *PLoS One*. 2014; 9(3):e90575. Epub 2014/03/05. <https://doi.org/10.1371/journal.pone.0090575> PMID: 24599287.
72. Balanathan P, Williams ED, Wang H, Pedersen JS, Horvath LG, Achen MG, et al. Elevated level of inhibin-alpha subunit is pro-tumourigenic and pro-metastatic and associated with extracapsular spread in advanced prostate cancer. *Br J Cancer*. 2009; 100(11):1784–93. Epub 2009/05/12. <https://doi.org/10.1038/sj.bjc.6605089> PMID: 19436293.
73. Mom CH, Engelen MJ, Willemse PH, Gietema JA, ten Hoor KA, de Vries EG, et al. Granulosa cell tumors of the ovary: the clinical value of serum inhibin A and B levels in a large single center cohort. *Gynecol Oncol*. 2007; 105(2):365–72. Epub 2007/02/15. <https://doi.org/10.1016/j.ygyno.2006.12.034> PMID: 17306349.
74. A Study of TRC105 in Combination With Paclitaxel/Carboplatin and Bevacizumab in Non-Squamous Cell Lung Cancer. <https://ClinicalTrials.gov/show/NCT02429843>.
75. Sorafenib and TRC105 in Hepatocellular Cancer. <https://ClinicalTrials.gov/show/NCT01306058>.
76. Trial of TRC105 and Sorafenib in Patients With HCC. <https://ClinicalTrials.gov/show/NCT02560779>.
77. TRC105 for Recurrent Glioblastoma. <https://ClinicalTrials.gov/show/NCT01778530>.
78. Study of TRC105 and Bevacizumab in Patients With Refractory Gestational Trophoblastic Neoplasia (GTN). <https://ClinicalTrials.gov/show/NCT02664961>.
79. Study of TRC105 Combined With Standard-Dose Bevacizumab for Advanced Solid Tumors for Which Bevacizumab is Indicated. <https://ClinicalTrials.gov/show/NCT01332721>.
80. TRC105 in Adults With Advanced/Metastatic Urothelial Carcinoma. <https://ClinicalTrials.gov/show/NCT01328574>.
81. Open Label Dose-Finding Study of TRC105 Plus Capecitabine for Metastatic Breast Cancer. <https://ClinicalTrials.gov/show/NCT01326481>.
82. Preoperative Combination of Letrozole, Everolimus, and TRC105 in Postmenopausal Hormone-Receptor Positive and Her2 Negative Breast Cancer. <https://ClinicalTrials.gov/show/NCT02520063>.
83. Study of TRC105 + Paclitaxel/Carboplatin and Bevacizumab in Patients With NSCLC. <https://ClinicalTrials.gov/show/NCT03780010>.
84. TRC105 for Liver Cancer That Has Not Responded to Sorafenib. <https://ClinicalTrials.gov/show/NCT01375569>.
85. A Phase 1B Dose-escalation and Phase 2a Study of Carotuximab (TRC105) in Combination With Pazopanib in Patients With Advanced Soft Tissue Sarcoma. <https://ClinicalTrials.gov/show/NCT01975519>.
86. TRC105 Combined With Standard-dose Bevacizumab for Two Patients With Metastatic And Refractory Choriocarcinoma. <https://ClinicalTrials.gov/show/NCT02396511>.
87. Trial of TRC105 and Pazopanib Versus Pazopanib Alone in Patients With Advanced Angiosarcoma. <https://ClinicalTrials.gov/show/NCT02979899>.
88. A Randomized Phase 2 Trial of Axitinib and TRC105 Versus Axitinib Alone in Patients With Advanced or Metastatic Renal Cell Carcinoma. <https://ClinicalTrials.gov/show/NCT01806064>.
89. Open Label Phase 1 Dose Finding Study of TRC105 in Patients With Solid Cancer. <https://ClinicalTrials.gov/show/NCT00582985>.

90. Study of TRC105 With Abiraterone and With Enzalutamide in Prostate Cancer Patients Progressing on Therapy. <https://ClinicalTrials.gov/show/NCT03418324>.
91. Study of Carotuximab (TRC105) Plus Nivolumab in Patients With Metastatic NSCLC. <https://ClinicalTrials.gov/show/NCT03181308>.
92. Bevacizumab With or Without TRC105 in Treating Patients With Metastatic Kidney Cancer. <https://ClinicalTrials.gov/show/NCT01727089>.
93. Evaluation of TRC105 in the Treatment of Recurrent Ovarian, Fallopian Tube, or Primary Peritoneal Carcinoma. <https://ClinicalTrials.gov/show/NCT01381861>.
94. A Phase I/II Study of TRC105 in Metastatic Castrate Resistant Prostate Cancer (CRPC). <https://ClinicalTrials.gov/show/NCT01090765>.
95. Open Label Continuation Study of TRC105 for Patients Who Have Completed a Prior TRC105 Trial. <https://ClinicalTrials.gov/show/NCT02354612>.
96. A Phase 2 Evaluation of TRC105 In Combination With Bevacizumab in Patients With Glioblastoma. <https://ClinicalTrials.gov/show/NCT01564914>.
97. Bevacizumab With or Without Anti-Endoglin Monoclonal Antibody TRC105 in Treating Patients With Recurrent Glioblastoma Multiforme. <https://ClinicalTrials.gov/show/NCT01648348>.
98. Schoonderwoerd MJ, Koops MF, Angela RA, Koolmoes B, Toitou M, Paauwe M, et al. Targeting endoglin expressing regulatory T cells in the tumor microenvironment enhances the effect of PD1 checkpoint inhibitor immunotherapy. *Clin Cancer Res*. 2020. Epub 2020/04/24. <https://doi.org/10.1158/1078-0432.CCR-19-2889> PMID: 32332012.
99. Bandyopadhyay A, Wang L, López-Casillas F, Mendoza V, Yeh IT, Sun L. Systemic administration of a soluble betaglycan suppresses tumor growth, angiogenesis, and matrix metalloproteinase-9 expression in a human xenograft model of prostate cancer. *Prostate*. 2005; 63(1):81–90. <https://doi.org/10.1002/pros.20166> PMID: 15468171.
100. Dong M, How T, Kirkbride KC, Gordon KJ, Lee JD, Hempel N, et al. The type III TGF-beta receptor suppresses breast cancer progression. *J Clin Invest*. 2007; 117(1):206–17. Epub 2006/12/07. <https://doi.org/10.1172/JCI29293> PMID: 17160136.
101. Naumann U, Maass P, Gleske AK, Aulwurf S, Weller M, Eisele G. Glioma gene therapy with soluble transforming growth factor-beta receptors II and III. *Int J Oncol*. 2008; 33(4):759–65. PMID: 18813789.
102. Finger EC, Turley RS, Dong M, How T, Fields TA, Blobel GC. TbetaRIII suppresses non-small cell lung cancer invasiveness and tumorigenicity. *Carcinogenesis*. 2008; 29(3):528–35. Epub 2008/01/03. <https://doi.org/10.1093/carcin/bgm289> PMID: 18174241.
103. Bandyopadhyay A, López-Casillas F, Malik SN, Montiel JL, Mendoza V, Yang J, et al. Antitumor activity of a recombinant soluble betaglycan in human breast cancer xenograft. *Cancer Res*. 2002; 62(16):4690–5. PMID: 12183427.
104. Lee JD, Hempel N, Lee NY, Blobel GC. The type III TGF-beta receptor suppresses breast cancer progression through GIPC-mediated inhibition of TGF-beta signaling. *Carcinogenesis*. 2010; 31(2):175–83. Epub 2009/12/02. <https://doi.org/10.1093/carcin/bgp271> PMID: 19955393.
105. Gallo-Oller G, Vollmann-Zwerenz A, Meléndez B, Rey JA, Hau P, Dotor J, et al. P144, a Transforming Growth Factor beta inhibitor peptide, generates antitumoral effects and modifies SMAD7 and SKI levels in human glioblastoma cell lines. *Cancer Lett*. 2016; 381(1):67–75. Epub 2016/07/26. <https://doi.org/10.1016/j.canlet.2016.07.029> PMID: 27473823.
106. Llopiz D, Dotor J, Casares N, Bezunartea J, Díaz-Valdés N, Ruiz M, et al. Peptide inhibitors of transforming growth factor-beta enhance the efficacy of antitumor immunotherapy. *Int J Cancer*. 2009; 125(11):2614–23. <https://doi.org/10.1002/ijc.24656> PMID: 19530254.
107. Gao J, Aksoy BA, Dogrusoz U, Dresdner G, Gross B, Sumer SO, et al. Integrative analysis of complex cancer genomics and clinical profiles using the cBioPortal. *Sci Signal*. 2013; 6(269):p1. Epub 2013/04/04. <https://doi.org/10.1126/scisignal.2004088> PMID: 23550210.
108. Cerami E, Gao J, Dogrusoz U, Gross BE, Sumer SO, Aksoy BA, et al. The cBio cancer genomics portal: an open platform for exploring multidimensional cancer genomics data. *Cancer Discov*. 2012; 2(5):401–4. Epub 2012/05/17. <https://doi.org/10.1158/2159-8290.CD-12-0095> PMID: 22588877.
109. Nagy Á, Lánckzy A, Menyhárt O, Gyórfy B. Validation of miRNA prognostic power in hepatocellular carcinoma using expression data of independent datasets. *Sci Rep*. 2018; 8(1):9227. Epub 2018/06/15. <https://doi.org/10.1038/s41598-018-27521-y> PMID: 29907753.
110. Fekete JT, Gyórfy B. ROCplot.org: Validating predictive biomarkers of chemotherapy/hormonal therapy/anti-HER2 therapy using transcriptomic data of 3,104 breast cancer patients. *Int J Cancer*. 2019; 145(11):3140–51. Epub 2019/04/26. <https://doi.org/10.1002/ijc.32369> PMID: 31020993.

111. Oughtred R, Stark C, Breitkreutz BJ, Rust J, Boucher L, Chang C, et al. The BioGRID interaction database: 2019 update. *Nucleic Acids Res.* 2019; 47(D1):D529–D41. <https://doi.org/10.1093/nar/gky1079> PMID: 30476227.
112. Huang da W, Sherman BT, Lempicki RA. Systematic and integrative analysis of large gene lists using DAVID bioinformatics resources. *Nat Protoc.* 2009; 4(1):44–57. Epub 2009/01/10. <https://doi.org/10.1038/nprot.2008.211> PMID: 19131956.
113. Broad D. DepMap 20Q1 Public2020.
114. Katayama Y, Oshima T, Sakamaki K, Aoyama T, Sato T, Masudo K, et al. Clinical Significance of. *In Vivo.* 2017; 31(4):565–71. <https://doi.org/10.21873/invivo.11095> PMID: 28652421.
115. Xiong S, Klausen C, Cheng JC, Zhu H, Leung PC. Activin B induces human endometrial cancer cell adhesion, migration and invasion by up-regulating integrin $\beta 3$ via SMAD2/3 signaling. *Oncotarget.* 2015; 6(31):31659–73. <https://doi.org/10.18632/oncotarget.5229> PMID: 26384307.
116. Kita A, Kasamatsu A, Nakashima D, Endo-Sakamoto Y, Ishida S, Shimizu T, et al. Activin B Regulates Adhesion, Invasiveness, and Migratory Activities in Oral Cancer: a Potential Biomarker for Metastasis. *J Cancer.* 2017; 8(11):2033–41. Epub 2017/07/05. <https://doi.org/10.7150/jca.18714> PMID: 28819404.
117. Chen ZL, Qin L, Peng XB, Hu Y, Liu B. INHBA gene silencing inhibits gastric cancer cell migration and invasion by impeding activation of the TGF- β signaling pathway. *J Cell Physiol.* 2019; 234(10):18065–74. Epub 2019/04/08. <https://doi.org/10.1002/jcp.28439> PMID: 30963572.
118. Li Y, Fortin J, Ongaro L, Zhou X, Boehm U, Schneyer A, et al. Betaglycan (TGFBR3) Functions as an Inhibin A, but Not Inhibin B, Coreceptor in Pituitary Gonadotrope Cells in Mice. *Endocrinology.* 2018; 159(12):4077–91. <https://doi.org/10.1210/en.2018-00770> PMID: 30364975.
119. Mankanji Y, Harrison CA, Stanton PG, Krishna R, Robertson DM. Inhibin A and B in vitro bioactivities are modified by their degree of glycosylation and their affinities to betaglycan. *Endocrinology.* 2007; 148(5):2309–16. Epub 2007/02/01. <https://doi.org/10.1210/en.2006-1612> PMID: 17272393.
120. Mankanji Y, Walton KL, Wilce MC, Chan KL, Robertson DM, Harrison CA. Suppression of inhibin A biological activity by alterations in the binding site for betaglycan. *J Biol Chem.* 2008; 283(24):16743–51. Epub 2008/04/07. <https://doi.org/10.1074/jbc.M801045200> PMID: 18397882.
121. Wiater E, Lewis KA, Donaldson C, Vaughan J, Bilezikjian L, Vale W. Endogenous betaglycan is essential for high-potency inhibin antagonism in gonadotropes. *Mol Endocrinol.* 2009; 23(7):1033–42. Epub 2009/04/16. <https://doi.org/10.1210/me.2009-0021> PMID: 19372236.
122. Mellor SL, Cranfield M, Ries R, Pedersen J, Cancilla B, de Kretser D, et al. Localization of activin beta (A)-, beta(B)-, and beta(C)-subunits in human prostate and evidence for formation of new activin heterodimers of beta(C)-subunit. *J Clin Endocrinol Metab.* 2000; 85(12):4851–8. <https://doi.org/10.1210/jcem.85.12.7052> PMID: 11134153.
123. Meyers RM, Bryan JG, McFarland JM, Weir BA, Sizemore AE, Xu H, et al. Computational correction of copy number effect improves specificity of CRISPR-Cas9 essentiality screens in cancer cells. *Nat Genet.* 2017; 49(12):1779–84. Epub 2017/10/30. <https://doi.org/10.1038/ng.3984> PMID: 29083409.
124. Dempster JM, Rossen J, Kazachkova M, Pan J, Kugener G, Root DE, et al. Extracting Biological Insights from the Project Achilles Genome-Scale CRISPR Screens in Cancer Cell Lines. *bioRxiv.* 2019:720243. <https://doi.org/10.1101/720243>
125. Ghandi M, Huang FW, Jané-Valbuena J, Kryukov GV, Lo CC, McDonald ER, et al. Next-generation characterization of the Cancer Cell Line Encyclopedia. *Nature.* 2019; 569(7757):503–8. Epub 2019/05/08. <https://doi.org/10.1038/s41586-019-1186-3> PMID: 31068700.
126. Tsherniak A, Vazquez F, Montgomery PG, Weir BA, Kryukov G, Cowley GS, et al. Defining a Cancer Dependency Map. *Cell.* 2017; 170(3):564–76.e16. <https://doi.org/10.1016/j.cell.2017.06.010> PMID: 28753430.
127. Nishida J, Miyazono K, Ehata S. Decreased TGFBR3/betaglycan expression enhances the metastatic abilities of renal cell carcinoma cells through TGF- β -dependent and -independent mechanisms. *Oncogene.* 2018; 37(16):2197–212. Epub 2018/02/02. <https://doi.org/10.1038/s41388-017-0084-0> PMID: 29391598.
128. Frias AE, Li H, Keeney GL, Podratz KC, Woodruff TK. Preoperative serum level of inhibin A is an independent prognostic factor for the survival of postmenopausal women with epithelial ovarian carcinoma. *Cancer.* 1999; 85(2):465–71. [https://doi.org/10.1002/\(sici\)1097-0142\(19990115\)85:2<465::aid-cnrcr26>3.0.co;2-w](https://doi.org/10.1002/(sici)1097-0142(19990115)85:2<465::aid-cnrcr26>3.0.co;2-w) PMID: 10023716.
129. Bashir M, Damineni S, Mukherjee G, Kondaiah P. Activin-A signaling promotes epithelial-mesenchymal transition, invasion, and metastatic growth of breast cancer. *NPJ Breast Cancer.* 2015; 1:15007. Epub 2015/08/12. <https://doi.org/10.1038/npjbcancer.2015.7> PMID: 28721365.

130. Okano M, Yamamoto H, Ohkuma H, Kano Y, Kim H, Nishikawa S, et al. Significance of INHBA expression in human colorectal cancer. *Oncol Rep*. 2013; 30(6):2903–8. Epub 2013/10/01. <https://doi.org/10.3892/or.2013.2761> PMID: 24085226.
131. Abrahao-Machado LF, Scapulatempo-Neto C. HER2 testing in gastric cancer: An update. *World J Gastroenterol*. 2016; 22(19):4619–25. <https://doi.org/10.3748/wjg.v22.i19.4619> PMID: 27217694.
132. Kim SK, Whitley MJ, Krzysiak TC, Hinck CS, Taylor AB, Zwieb C, et al. Structural Adaptation in Its Orphan Domain Engenders Betaglycan with an Alternate Mode of Growth Factor Binding Relative to Endoglin. *Structure*. 2019; 27(9):1427–42.e4. Epub 2019/07/18. <https://doi.org/10.1016/j.str.2019.06.010> PMID: 31327662.
133. Chang HY, Nuyten DS, Sneddon JB, Hastie T, Tibshirani R, Sørli T, et al. Robustness, scalability, and integration of a wound-response gene expression signature in predicting breast cancer survival. *Proc Natl Acad Sci U S A*. 2005; 102(10):3738–43. Epub 2005/02/08. <https://doi.org/10.1073/pnas.0409462102> PMID: 15701700.
134. Haider S, Wang J, Nagano A, Desai A, Arumugam P, Dumartin L, et al. A multi-gene signature predicts outcome in patients with pancreatic ductal adenocarcinoma. *Genome Med*. 2014; 6(12):105. Epub 2014/12/03. <https://doi.org/10.1186/s13073-014-0105-3> PMID: 25587357.
135. Hallett RM, Dvorkin-Gheva A, Bane A, Hassell JA. A gene signature for predicting outcome in patients with basal-like breast cancer. *Sci Rep*. 2012; 2:227. Epub 2012/01/17. <https://doi.org/10.1038/srep00227> PMID: 22355741.
136. Kim SY, Kim YS. A gene sets approach for identifying prognostic gene signatures for outcome prediction. *BMC Genomics*. 2008; 9:177. Epub 2008/04/16. <https://doi.org/10.1186/1471-2164-9-177> PMID: 18416850.
137. Kanehisa M, Goto S. KEGG: kyoto encyclopedia of genes and genomes. *Nucleic Acids Res*. 2000; 28(1):27–30. <https://doi.org/10.1093/nar/28.1.27> PMID: 10592173.
138. Massagué J. TGFbeta in Cancer. *Cell*. 2008; 134(2):215–30. <https://doi.org/10.1016/j.cell.2008.07.001> PMID: 18662538.
139. Baldewijns MM, Thijssen VL, Van den Eynden GG, Van Laere SJ, Bluekens AM, Roskams T, et al. High-grade clear cell renal cell carcinoma has a higher angiogenic activity than low-grade renal cell carcinoma based on histomorphological quantification and qRT-PCR mRNA expression profile. *Br J Cancer*. 2007; 96(12):1888–95. Epub 2007/05/15. <https://doi.org/10.1038/sj.bjc.6603796> PMID: 17505508.
140. Das S, Marsden PA. Angiogenesis in glioblastoma. *N Engl J Med*. 2013; 369(16):1561–3. <https://doi.org/10.1056/NEJMcibr1309402> PMID: 24131182.
141. Longui CA, Lemos-Marini SH, Figueiredo B, Mendonca BB, Castro M, Liberatore R, et al. Inhibin alpha-subunit (INH A) gene and locus changes in paediatric adrenocortical tumours from TP53 R337H mutation heterozygote carriers. *J Med Genet*. 2004; 41(5):354–9. <https://doi.org/10.1136/jmg.2004.018978> PMID: 15121773.
142. Tremblay JJ, Viger RS. GATA factors differentially activate multiple gonadal promoters through conserved GATA regulatory elements. *Endocrinology*. 2001; 142(3):977–86. <https://doi.org/10.1210/endo.142.3.7995> PMID: 11181509.
143. Gong Y, Zhang L, Zhang A, Chen X, Gao P, Zeng Q. GATA4 inhibits cell differentiation and proliferation in pancreatic cancer. *PLoS One*. 2018; 13(8):e0202449. Epub 2018/08/24. <https://doi.org/10.1371/journal.pone.0202449> PMID: 30142155.
144. Han Q, Xu X, Li J, Wang J, Bai L, Wang A, et al. GATA4 is highly expressed in childhood acute lymphoblastic leukemia, promotes cell proliferation and inhibits apoptosis by activating BCL2 and MDM2. *Mol Med Rep*. 2017; 16(5):6290–8. Epub 2017/08/28. <https://doi.org/10.3892/mmr.2017.7369> PMID: 28849107.
145. Nikiteas NI, Tzanakis N, Theodoropoulos G, Atsaves V, Christoni Z, Karakitsos P, et al. Vascular endothelial growth factor and endoglin (CD-105) in gastric cancer. *Gastric Cancer*. 2007; 10(1):12–7. Epub 2007/02/23. <https://doi.org/10.1007/s10120-006-0401-8> PMID: 17334712.
146. Chen C-Y, Sheu M-J. Endoglin targeting inhibits tumor angiogenesis in non-small cell lung cancer. *The FASEB Journal*. 2018; 32(1_supplement):695.16–16. https://doi.org/10.1096/fasebj.2018.32.1_supplement.695.16
147. Henry LA, Johnson DA, Sarrió D, Lee S, Quinlan PR, Crook T, et al. Endoglin expression in breast tumor cells suppresses invasion and metastasis and correlates with improved clinical outcome. *Oncogene*. 2011; 30(9):1046–58. Epub 2010/11/01. <https://doi.org/10.1038/onc.2010.488> PMID: 21042283.
148. Kauer J, Schwartz K, Tandler C, Hinterleitner C, Roerden M, Jung G, et al. CD105 (Endoglin) as negative prognostic factor in AML. *Sci Rep*. 2019; 9(1):18337. Epub 2019/12/04. <https://doi.org/10.1038/s41598-019-54767-x> PMID: 31797971.

149. Bhola NE, Balko JM, Dugger TC, Kuba MG, Sánchez V, Sanders M, et al. TGF- β inhibition enhances chemotherapy action against triple-negative breast cancer. *J Clin Invest*. 2013; 123(3):1348–58. Epub 2013/02/08. <https://doi.org/10.1172/JCI65416> PMID: 23391723.
150. Vogiatzi F, Brandt DT, Schneikert J, Fuchs J, Grikscheit K, Wanzel M, et al. Mutant p53 promotes tumor progression and metastasis by the endoplasmic reticulum UDPase ENTPD5. *Proc Natl Acad Sci U S A*. 2016; 113(52):E8433–E42. Epub 2016/12/12. <https://doi.org/10.1073/pnas.1612711114> PMID: 27956623.
151. Kirkbride KC, Ray BN, Blobbe GC. Cell-surface co-receptors: emerging roles in signaling and human disease. *Trends Biochem Sci*. 2005; 30(11):611–21. Epub 2005/09/28. <https://doi.org/10.1016/j.tibs.2005.09.003> PMID: 16185874.
152. Knelson EH, Gaviglio AL, Tewari AK, Armstrong MB, Myhre K, Blobbe GC. Type III TGF-beta receptor promotes FGF2-mediated neuronal differentiation in neuroblastoma. *J Clin Invest*. 2013; 123(11):4786–98. Epub 2013/11/13. <https://doi.org/10.1172/JCI69657> PMID: 24216509.
153. Jenkins LM, Singh P, Varadaraj A, Lee NY, Shah S, Flores HV, et al. Altering the Proteoglycan State of Transforming Growth Factor beta Type III Receptor (TbetaRIII)/Betaglycan Modulates Canonical Wnt/beta-Catenin Signaling. *J Biol Chem*. 2016; 291(49):25716–28. Epub 2016/10/28. <https://doi.org/10.1074/jbc.M116.748624> PMID: 27784788.
154. Moyano-Galceran L, Pietilä EA, Turunen SP, Corvigno S, Hjerpe E, Bulanova D, et al. Adaptive RSK-EphA2-GPRC5A signaling switch triggers chemotherapy resistance in ovarian cancer. *EMBO Mol Med*. 2020; 12(4):e11177. Epub 2020/03/02. <https://doi.org/10.15252/emmm.201911177> PMID: 32115889.
155. De Robertis M, Loiacono L, Fusilli C, Poeta ML, Mazza T, Sanchez M, et al. Dysregulation of EGFR Pathway in EphA2 Cell Subpopulation Significantly Associates with Poor Prognosis in Colorectal Cancer. *Clin Cancer Res*. 2017; 23(1):159–70. Epub 2016/07/11. <https://doi.org/10.1158/1078-0432.CCR-16-0709> PMID: 27401248.
156. Zhuang G, Brantley-Sieders DM, Vaught D, Yu J, Xie L, Wells S, et al. Elevation of receptor tyrosine kinase EphA2 mediates resistance to trastuzumab therapy. *Cancer Res*. 2010; 70(1):299–308. Epub 2009/12/22. <https://doi.org/10.1158/0008-5472.CAN-09-1845> PMID: 20028874.
157. Huang J, Xiao D, Li G, Ma J, Chen P, Yuan W, et al. EphA2 promotes epithelial-mesenchymal transition through the Wnt/ β -catenin pathway in gastric cancer cells. *Oncogene*. 2014; 33(21):2737–47. Epub 2013/06/10. <https://doi.org/10.1038/onc.2013.238> PMID: 23752181.
158. Kim CY, Oh JH, Lee JY, Kim MH. The LncRNA HOTAIRM1 Promotes Tamoxifen Resistance by Mediating HOXA1 Expression in ER+ Breast Cancer Cells. *J Cancer*. 2020; 11(12):3416–23. Epub 2020/03/13. <https://doi.org/10.7150/jca.38728> PMID: 32284737.
159. Bitu CC, Destro MF, Carrera M, da Silva SD, Graner E, Kowalski LP, et al. HOXA1 is overexpressed in oral squamous cell carcinomas and its expression is correlated with poor prognosis. *BMC Cancer*. 2012; 12:146. Epub 2012/04/12. <https://doi.org/10.1186/1471-2407-12-146> PMID: 22498108.
160. Wardwell-Ozgo J, Dogruluk T, Gifford A, Zhang Y, Heffernan TP, van Doorn R, et al. HOXA1 drives melanoma tumor growth and metastasis and elicits an invasion gene expression signature that prognosticates clinical outcome. *Oncogene*. 2014; 33(8):1017–26. Epub 2013/02/25. <https://doi.org/10.1038/onc.2013.30> PMID: 23435427.
161. Zimmer BM, Howell ME, Wei Q, Ma L, Romsdahl T, Loughman EG, et al. Loss of exogenous androgen dependence by prostate tumor cells is associated with elevated glucuronidation potential. *Horm Cancer*. 2016; 7(4):260–71. Epub 2016/06/15. <https://doi.org/10.1007/s12672-016-0268-z> PMID: 27307252.
162. Allain EP, Rouleau M, Lévesque E, Guillemette C. Emerging roles for UDP-glucuronosyltransferases in drug resistance and cancer progression. *Br J Cancer*. 2020; 122(9):1277–87. Epub 2020/02/12. <https://doi.org/10.1038/s41416-019-0722-0> PMID: 32047295.
163. Gummow BM, Winnay JN, Hammer GD. Convergence of Wnt signaling and steroidogenic factor-1 (SF-1) on transcription of the rat inhibin alpha gene. *J Biol Chem*. 2003; 278(29):26572–9. Epub 2003/05/05. <https://doi.org/10.1074/jbc.M212677200> PMID: 12732619.
164. de la Fuente-Granada M, Olguin-Alor R, Ortega-Francisco S, Bonifaz LC, Soldevila G. Inhibins regulate peripheral regulatory T cell induction through modulation of dendritic cell function. *FEBS Open Bio*. 2019; 9(1):137–47. Epub 2018/12/11. <https://doi.org/10.1002/2211-5463.12555> PMID: 30652081.
165. Li J, Wang H, Li Z, Zhang C, Li C, Yu H. A 5-Gene Signature Is Closely Related to Tumor Immune Microenvironment and Predicts the Prognosis of Patients with Non-Small Cell Lung Cancer. *Biomed Res Int*. 2020; 2020:2147397. Epub 2020/01/10. <https://doi.org/10.1155/2020/2147397> PMID: 31998783.

166. Ruiz EML, Niu T, Zerfaoui M, Kunnimalaiyaan M, Friedlander PL, Abdel-Mageed AB, et al. A novel gene panel for prediction of lymph-node metastasis and recurrence in patients with thyroid cancer. *Surgery*. 2020; 167(1):73–9. Epub 2019/11/09. <https://doi.org/10.1016/j.surg.2019.06.058> PMID: 31711617.
167. Yang H, Zhang X, Cai XY, Wen DY, Ye ZH, Liang L, et al. From big data to diagnosis and prognosis: gene expression signatures in liver hepatocellular carcinoma. *PeerJ*. 2017; 5:e3089. Epub 2017/03/14. <https://doi.org/10.7717/peerj.3089> PMID: 28316892.
168. Huang L, Zheng M, Zhou QM, Zhang MY, Yu YH, Yun JP, et al. Identification of a 7-gene signature that predicts relapse and survival for early stage patients with cervical carcinoma. *Med Oncol*. 2012; 29(4):2911–8. Epub 2012/01/25. <https://doi.org/10.1007/s12032-012-0166-3> PMID: 22274917.
169. Zhang YE. Non-Smad pathways in TGF-beta signaling. *Cell Res*. 2009; 19(1):128–39. Epub 2008/12/31. <https://doi.org/10.1038/cr.2008.328> PMID: 19114990.
170. Derynck R, Zhang YE. Smad-dependent and Smad-independent pathways in TGF-beta family signaling. *Nature*. 2003; 425(6958):577–84. Epub 2003/10/10. <https://doi.org/10.1038/nature02006> PMID: 14534577.
171. Torsney E, Charlton R, Parums D, Collis M, Arthur HM. Inducible expression of human endoglin during inflammation and wound healing in vivo. *Inflamm Res*. 2002; 51(9):464–70. <https://doi.org/10.1007/pl00012413> PMID: 12365720.
172. Alzahrani A, Chi Y, Finnson KW, Blati M, Lussier B, Kapoor M, et al. Endoglin haploinsufficiency is associated with differential regulation of extracellular matrix production during skin fibrosis and cartilage repair in mice. *J Cell Commun Signal*. 2018; 12(1):379–88. Epub 2018/02/27. <https://doi.org/10.1007/s12079-018-0461-7> PMID: 29488175.
173. Myhre K, Knelson EH, Gatzka CE, Gatzka ML, Globe GC. TβRIII/β-arrestin2 regulates integrin α5β1 trafficking, function, and localization in epithelial cells. *Oncogene*. 2013; 32(11):1416–27. Epub 2012/05/07. <https://doi.org/10.1038/onc.2012.157> PMID: 22562249.
174. Jarosz M, Jazowiecka-Rakus J, Cichoń T, Głowala-Kosińska M, Smolarczyk R, Smagur A, et al. Therapeutic antitumor potential of endoglin-based DNA vaccine combined with immunomodulatory agents. *Gene Ther*. 2013; 20(3):262–73. Epub 2012/04/12. <https://doi.org/10.1038/gt.2012.28> PMID: 22495576.